

LIERARY Michigan State University

This is to certify that the

thesis entitled

FINITE ELEMENT ANALYSIS OF NOTCHED SPECIMENS WITH EXPERIMENTAL VERIFICATION AT ROOM AND ELEVATED TEMPERATURES

presented by

MATTHEW E. MELIS

has been accepted towards fulfillment of the requirements for

MASTERS degree in MeCHANICS

Major professor

Date 10/28/13

MSU is an Affirmative Action/Equal Opportunity Institution

0-7639



RETURNING MATERIALS:
Place in book drop to remove this checkout from your record. FINES will be charged if book is returned after the date stamped below.

FINITE ELEMENT ANALYSIS OF NOTCHED SPECIMENS WITH EXPERIMENTAL VERIFICATION AT ROOM AND ELEVATED TEMPERATURES

Вy

Matthew E. Melis

A THESIS

Submitted to
Michigan State University
in partial fulfillment of the requirements
for the degree of

MASTER OF SCIENCE

Department of Metallurgy, Mechanics and Materials Science

1983

ABSTRACT

FINITE ELEMENT ANALYSIS OF NOTCHED SPECIMENS WITH EXPERIMENTAL VERIFICATION AT ROOM AND ELEVATED TEMPERATURES

Вy

Matthew E. Melis

tic, plastic, and creep solutions at room temperature and 1,200° F were observed under cyclic load conditions with hold times. Strains were measured at both local and remote regions of circular and elliptically notched specimens of cyclically stabilized Hastelloy X and local stress-strain response was predicted with good accuracy using smooth specimen simulation techniques. Load histories were reproduced on the computer for finite element analysis. Finite element analyses gave highly accurate results in predicting the stress and strain response at the notch of the notched members at room temperatures, however, a significant variance between experimental and analytical data was observed with results at 1,200° F.

ACKNOWLEDG MENTS

This thesis project was funded by the National Aeronautics and Space Administration.

I wish to express my sincere appreciation to my advisor, Dr. John Martin, for his support and encouragement throughout this work. Much thanks to Jim Oliver and the Case Center for their patience and assistance with my work on the computer. I would also like to thank Barry Spletzer, John Cuccio, and Goat for the insight, humor, and friendship they've extended towards me this last year. Finally, I want to give a very special thanks to my Mom and Dad, for none of this would have been possible without them.

TABLE OF CONTENTS

P	age
LIST OF TABLES	v
LIST OF FIGURES	vi
Chapter 1 INTRODUCTION	1
Chapter 2 NOTCHED GEOMETRIES AND MATERIAL	4
2.1 Specimen Configurations	4
2.2 Material	10
Chapter 3 EXPERIMENTAL TECHNIQUES	12
3.1 Strain Measurement with the ISG	12
3.2 Room Temperature Tests	13
3.3 Elevated Temperature Tests	13
3.4 Smooth Specimen Stress Simulation	17
Chapter 4 ANALYSIS	18
4.1 Analytical Methods	18
4.1.1 Elastic Analysis	23
4.1.2 Plastic Analysis	26
4.1.3 Creep Analysis	30
4.2 Computer Implementation	31
Chapter 5 RESULTS AND DISCUSSION	33
5.1 Linear Analysis	33
5.2 Nonlinear Analysis	36
5.2.1 Room Temperature	36
5.2.2 Elevated Temperature	42

																						Page
Chapter 6 CONCLUSIONS	•	•	•	•	•	•	•	•	•	•	•	•	•	•	•	•	•	•	•	•	•	47
LIST OF REFERENCES			_																			48

LIST OF TABLES

Table																		Page
1	Material Properties	•	•	•	•	•	•	•	•	•		•	•	•	•	•	•	11

LIST OF FIGURES

Figure		Page
1	Notched Specimen Geometry	6
2	Smooth Specimen Geometry	7
3	Notched Specimens	8
4	Smooth Specimens	9
5	Load Patterns With Typical Notch Root Strain Response.	14
6	Diametral Extensometer	16
7	Finite Element Grids	19
8	Axisymmetric Finite Element Representation	21
9	Two Dimensional Isoparametric Element	22
10	ANSYS oy Contour Plots	24
11	ANSYS Displacement Plots	25
12	Bilinear Kinematic Hardening Model	27
13	Bilinear Form of Stress Strain Response	27
14	Strain Energy Slope Determination	29
15	Stress Concentration Profiles of Notched Specimens	35
16	Hysteresis Loops of Smooth Specimen at	
	Room Temperature	37
17	Circular Notch Strain Versus Time at Room Temperature .	38
18	Elliptical Notch Strain Versus Time at	
	Room Temperature	39
19	Stress Versus Strain of Circular Notched Specimen at	
	Poor Terrescenture	40

Figure		Page
20	Stress Versus Strain of Elliptical Notched Specimen	
	at Room Temperature	41
21	Hysteresis Loops of Smooth Specimen at 1,200° F	43
22	Creep Response of Smooth Specimen Under	
	Constant Stress at 1,200° F	44
23	Strain Versus Time of Circular Notched Specimen	
	at 1,200° F	45
24	Stress Versus Strain of Circular Notched Specimen	
	at 1,200° F	46

CHAPTER 1

INTRODUCTION

Recent trends in the Aero-aircraft industries have been aimed towards developing more energy efficient propulsion systems. Increased efficiency results in higher operating temperatures, higher stresses, and more severe thermal gradients in the hot section components than ever before (1)*. These components such as turbine blades, vanes, and combustor liners would be typically fabricated from a high temperature super alloy such as the alloy Hastelloy X. In an effort to better understand the problems associated with material behavior in high temperature environments, experimental data have been collected in order to develop more reliable theoretical models for these materials. Accurate data of this type are not readily available.

A major part of this research has involved the turbine combustor (2,3). The liner of this combustor consists of multiple sheet metal louvers welded together to form a cylindrical structure. The combustor is cooled by air flow made possible by the inclusion of many holes in the liner so as to allow air to pass freely. These holes produce high stress concentrations at the notch which can ultimately result in crack initiation. Several constitutive relations have been developed to predict stress-strain response near these holes (1,4). The scope

^{*}Numbers in parenthesis refer to references listed in the reference table. Numbers in brackets refer to equations.

of this thesis is to utilize one of these methods, a nonlinear finite model (ANSYS), and the appropriate constitutive relations to predict the local stress-strain behavior in notched specimens of Hastelloy X. These predictions will then be compared to experimental data to determine the accuracy of the method.

The finite element method has played an important role in the analysis of hot section components in turbine engines (1-5). Finite elements were first initiated by an engineering group from the Boeing Corporation in attempts to develop a more advanced technique for the analysis of aircraft structures. Since then, the finite element method has evolved to the point where it can now be applied to a wide variety of engineering problems. The basic premise of this method is to make a discrete geometric model of the object being studied by creating a grid of elements and nodes to resemble the object itself. Boundary conditions are then imposed to simulate actual loading conditions and numerical integration techniques used within the computer program solve the problem.

Several finite element codes have been developed to date and are available on the commercial market such as NASTRAN, MARC, and ANSYS which was the code used for this study. Elasticity, plasticity and creep laws utilized within ANSYS are applied to elliptical and circular notch geometries.

Experimental data generated for comparison with the finite element results were obtained using a laser based interferometric strain gage (ISG). The ISG, developed by Dr. William Sharpe (6-9), was used throughout this study to measure notch root and remote strains on the notched specimens at both room temperature and 1,200° F.

Only strains can be directly measured in a notched plate. Stresses cannot be determined directly. Several researchers indicated that a smooth specimen could simulate the stress response in a notched member (10-13). This smooth specimen simulation was used in this work to estimate notch stress behavior.

CHAPTER 2

NOTCH GEOMETRIES AND MATERIAL

2.1 SPECIMEN CONFIGURATIONS

Members of constant cross section under load display uniformly stressed areas with a gradual change in stress contours. These configurations rarely exist however, in actual structural applications. The presence of notches and holes cause stress distributions resulting in high localized stresses. These areas are termed stress concentrations and are quantified by the stress concentration factor K_t . K_t is a theoretical or experimental value based on assumptions used in the theory of elasticity (14).

For members having holes, Peterson gives two types of stress concentration factors:

$$K_{tg} = \sigma_{max} / \sigma$$
 [1]

where: K_{tg} =stress concentration factor based on gross stress

 σ_{max} =maximum stress, at edge of hole

σ =applied stress, distant from hole

and

 $\mathbf{K}_{tn} = \sigma_{max} / \sigma_{nom} \tag{2}$

where: K_{tn} =stress concentration factor based on net (nominal) stress σ_{nom} =nominal (net) stress = $\sigma/(2-a/w)$

where: a=hole diameter
w=width of plate

As a result of high stresses near a hole, plastic deformation leading to crack initiation usually occurs in this reigon. This presents a significant problem for structural members containing holes.

A combustor for a turbine engine is such a structure. It has many holes in its liner to allow for the passage of air and gasses. To study the stress-strain occuring at this type of notch, thin plates with either a circular or elliptical centered notch were used to study this problem. From Peterson, theoretical elastic stress concentration factors were determined for the two notched geometries. K_{tg} [1] was given as 3.32 for the circular notch and 5.30 for the elliptical notch. These will be discussed in more detail in Chapter 4. Axial specimens were used to determine material properties and perform smooth specimen notch root stress simulation. Figures 1 through 4 show specimen drawings and photographs. All specimens were supplied by NASA and were made of Hastelloy X.

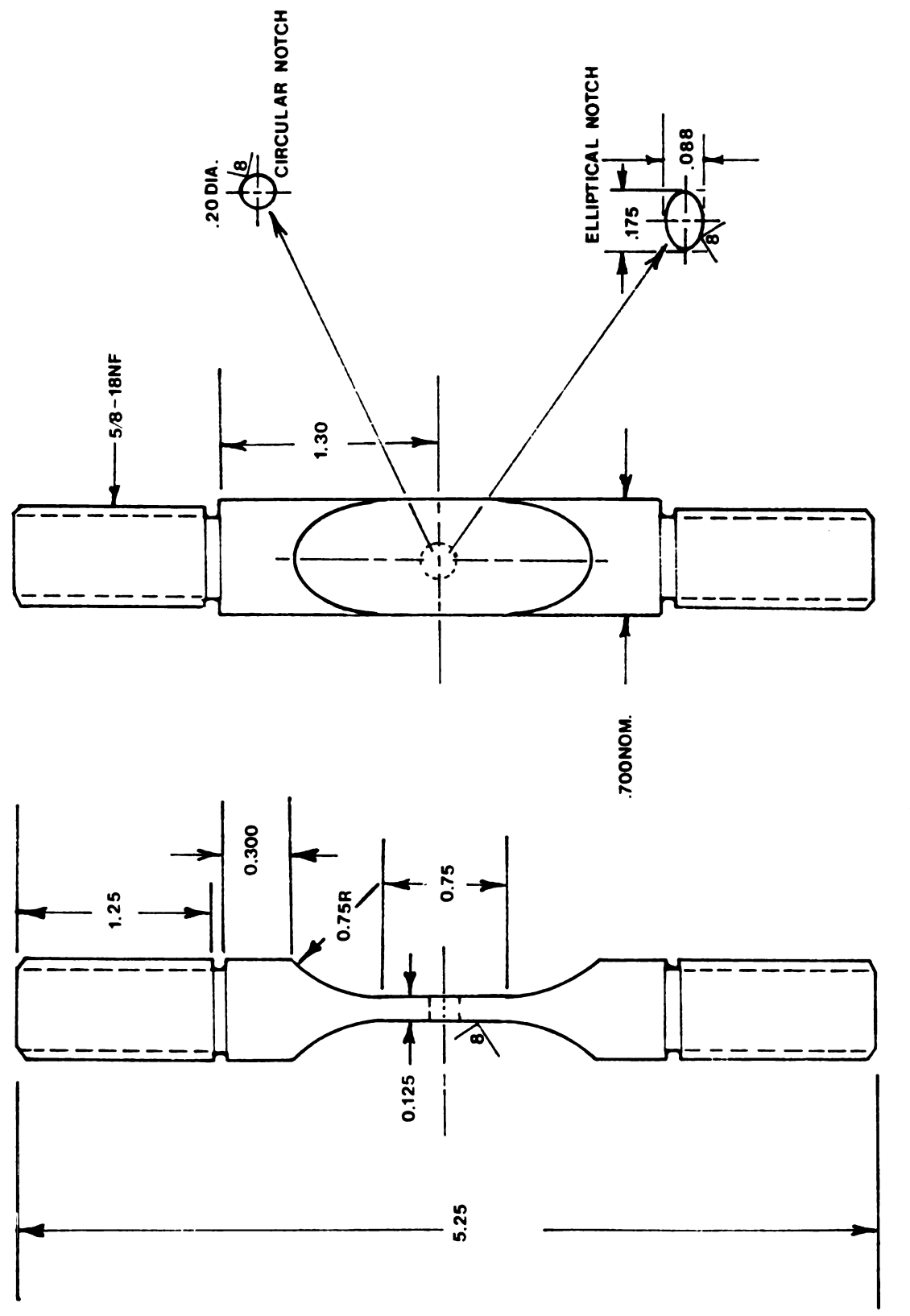
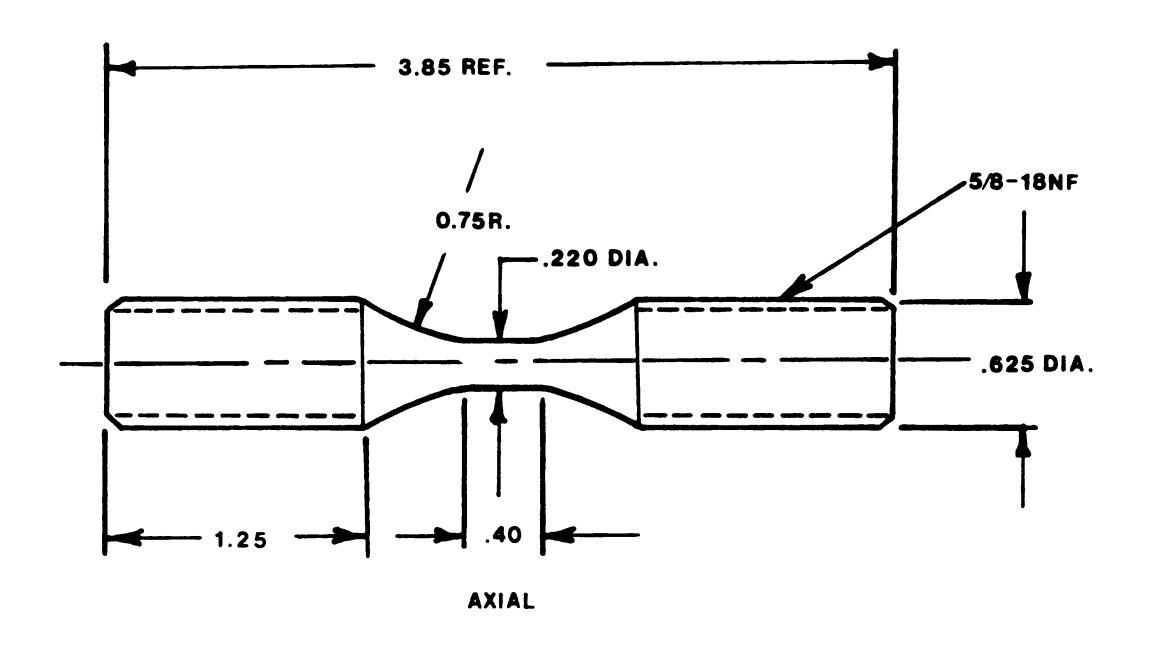


FIGURE 1 NOTCHED SPECIMEN GEOMETRY



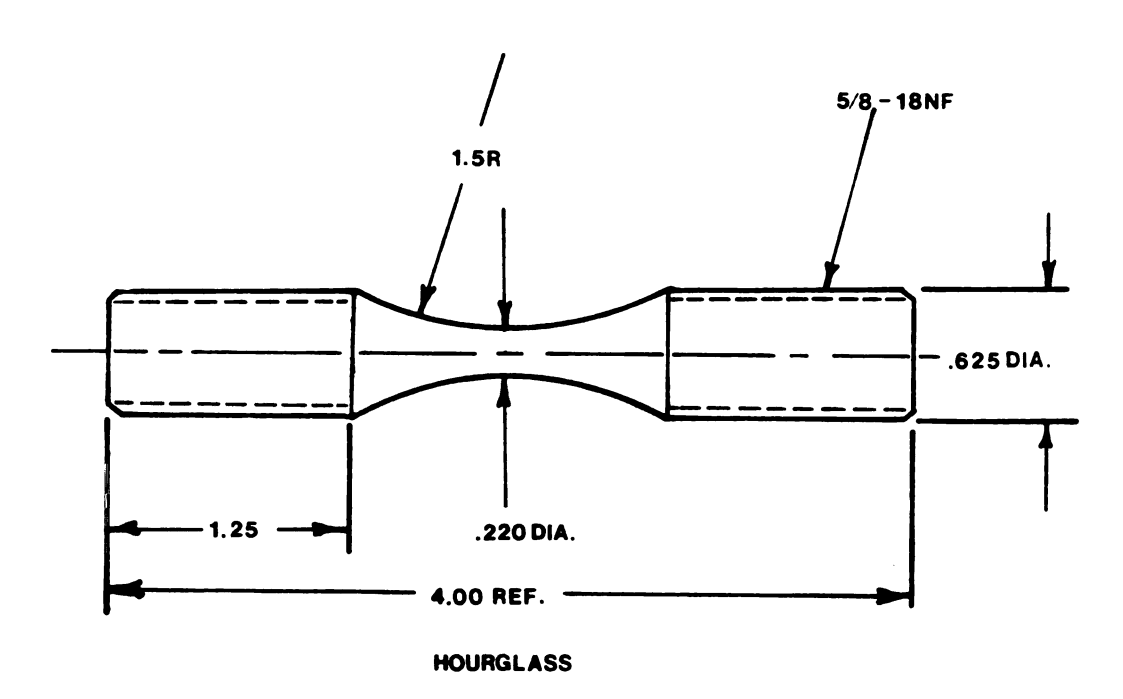


FIGURE 2 SMOOTH SPECIMEN GEOMETRY



FIGURE 3 NOTCHED SPECIMENS

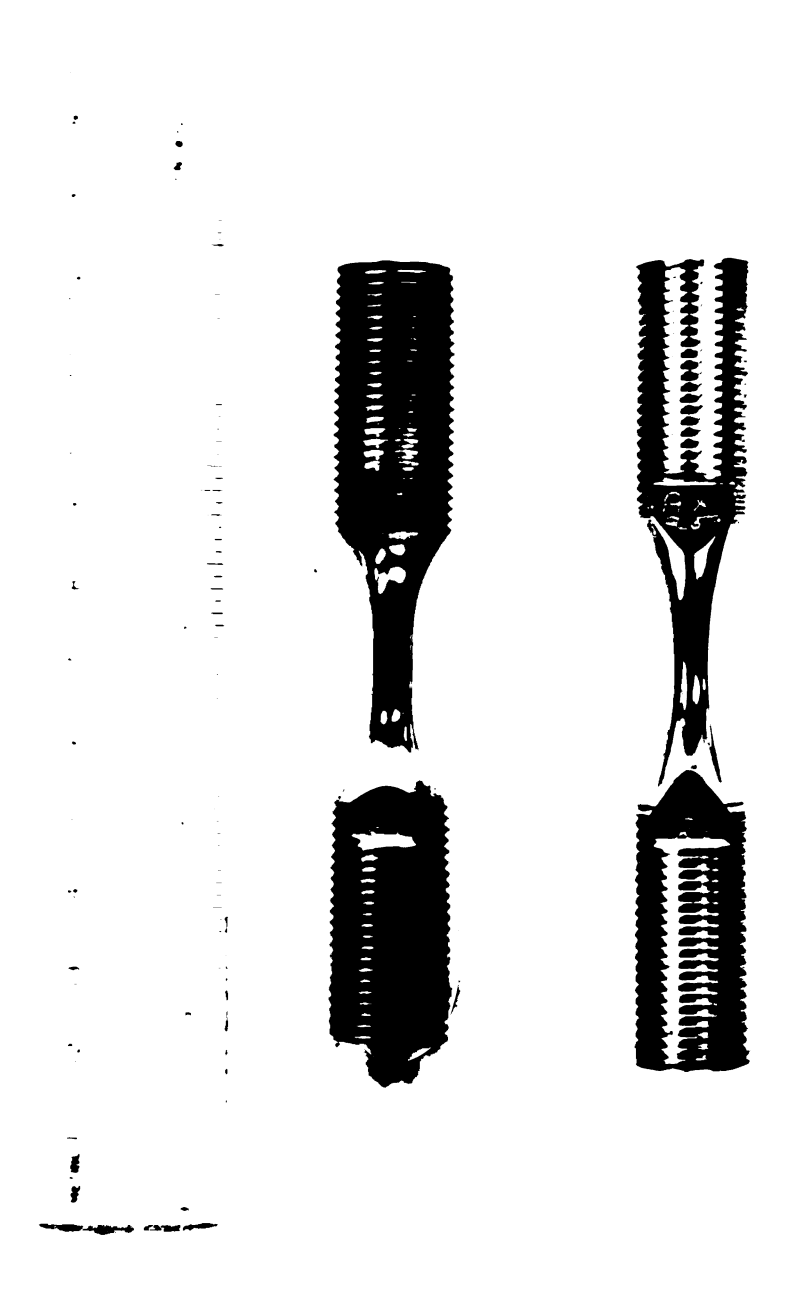


FIGURE 4 SMOOTH SPECIMENS

2.2 MATERIAL

Hastelloy X is a cyclicly hardening nickel base super alloy used for high temperature applications in furnaces, jet engines, and rocket motor parts. This metal has exceptional durability and possesses a strong oxidation resistance (up to 2,200°F) which makes it a good material for hot section applications. Material proporties pertinent to this project are given in Table 1. A more complete set of data of Hastelloy X proporties are given in reference (15).

Table 1. Material Properties

	Cest erature	Modulus of Elasticity	Poisson's Ratio		NSYS 1 Stress
°C	[°F]	MPa [ksi*10 ³]		MPa	[ksi]
25	[76]	182,718 [26.5]	.32	483	[70.0]
649	[1,200]	152,586 [22.1]	.34	403	[58.5]

CHAPTER 3

EXPERIMENTAL TECHNIQUES

3.1 STRAIN MEASUREMENT WITH THE ISG

Among the most recently developed high temperature testing instruments is the ISG. The two major advantages this technique has over conventional gages are the non-contacting nature of the device, and its ability to measure strains over a gage length of 50-100 microns, virtually measuring the strain at a point. The result is an accurate method of measuring strain response in non-uniform geometries.

The basic theory of the ISG involves creating a set of interference fringes by reflecting a laser beam off of two small pyramidal indentations put into the specimen with a vickers hardness tester. The indentations measure about 25 microns to a side and have been spaced 100 microns apart from center to center. The fringes are swept across a photomultiplier tube arrangement via a set of oscillating servo mirrors. Analog signals from the photomultiplier tubes are converted to digital signals and manipulated in a mini computer resulting in analog strain output. ISG calibration and experimental procedures that were used in this study can be found in Lucas (16), and Bofferding (17). All tests were performed on either an 11 Kip or a 55 Kip MTS closed loop test system. The specimens were mounted with a woods metal arrangement to avoid unwanted stresses that could result from the mounting procedure.

3.2 ROOM TEMPERATURE TESTS

Hastelloy X cyclically hardens but stabilizes very rapidly. This work was only concerned with stable cyclic response of the material. Each specimen was cycled untill its stable condition was attained before notch strain measurements were taken.

Smooth specimen tests at room temperature were performed on axial specimens with a straight gage section. A 0.3 inch MTS extensometer was used to determine pertinent material properties needed for the finite element model such as the modulus of elasticity and the strain hardening exponent. Some creep effects were observed at room temperature; however, they were not significant enough to be included in the model.

The next sequence of tests were run using the ISG to determine the elastic strain profiles along the notched section of both the elliptical and circular geometries for comparison to the finite element results. Being careful to stress the specimens only in the elastic range, readings were taken at five different points along the midspan of each specimen to determine the elastic strain response.

Testing done in the plastic range was performed under load control using a ramp function of 2.5×10^{-2} Hz. Maximum load being 3.5 Kips and 2.5 Kips for the circular and elliptical notched specimens respectively. Figure 5 depicts how the imposed load and the resulting strain response were recorded using a dual pen X-Y plotter on a time base sweep.

3.3 ELEVATED TEMPERATURE TESTS

Similar tests as described in section 3.2 were performed on specimens at 1,200° F taking note to observe time dependent effects at the higher temperature. It has been demonstrated that the ISG can measure

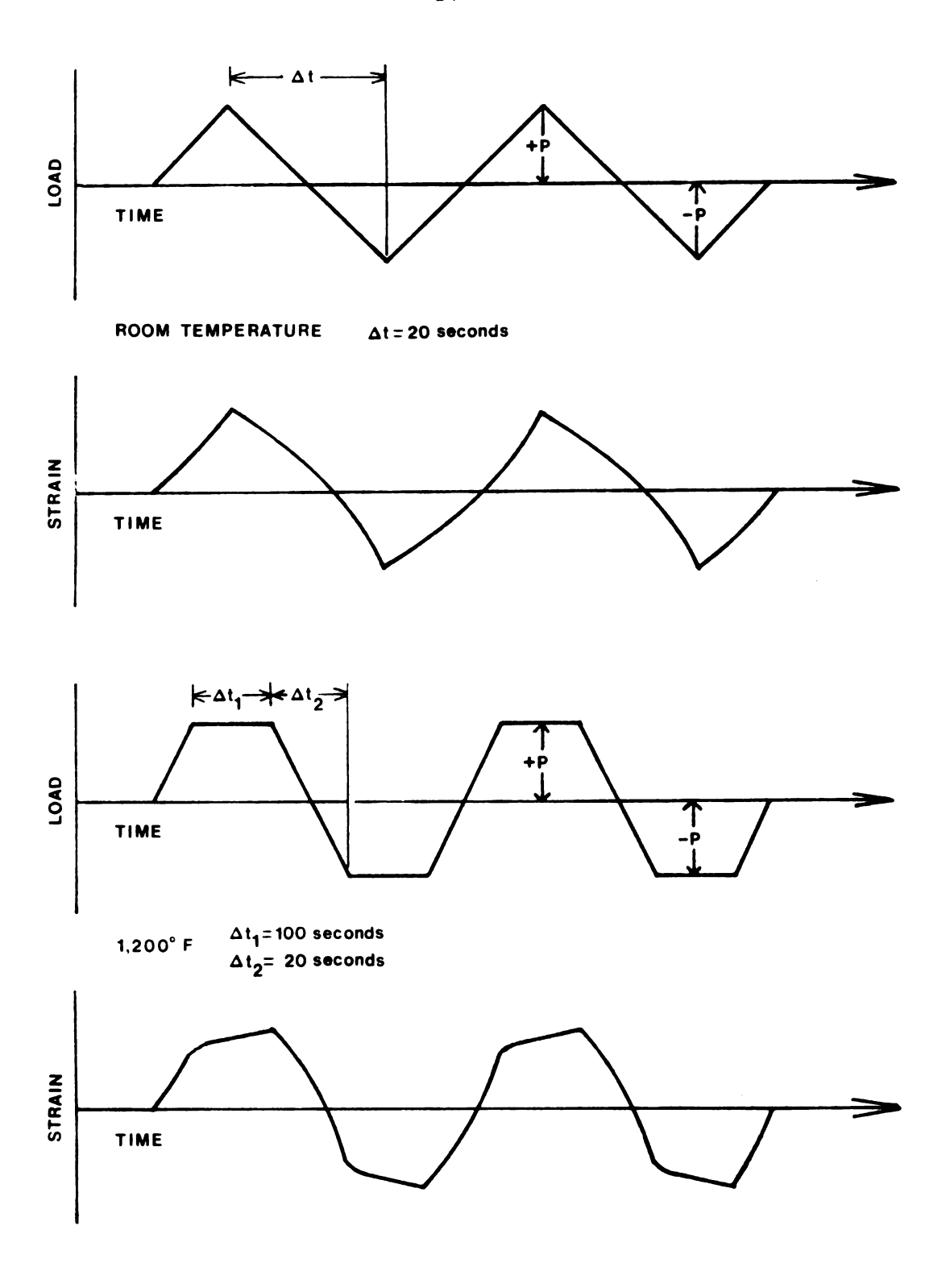


FIGURE 5 LOAD PATTERNS WITH TYPICAL NOTCH ROOT STRAIN RESPONSE

strains at temperatures up to 1,500° F; however, problems with surface oxidation and black body radiation become severe (16). To help alleviate this problem, even at 1,200° F, the notched specimens were plated with a layer of palladium-gold after the indenting procedures were completed. The palladium-gold coating retained its reflective ability for a long enough time so that accurate measurements could be taken to study the creep effects.

The basic setup was essentially the same for the room temperature and the elevated temperature tests except for some added preparation on the latter. Mounting the specimens involved careful centering of a copper induction coil so that no contact was made between the specimen and the coil and yet insuring the undisturbed passage of the interference fringes or the diameteral gage through the coil. A 5 KW induction heater was used to bring the specimens up to temperature. The temperature was controlled through a feedback signal via a thermocouple that was spot welded on the back side of the specimen.

Material properties were determined at 1,200° F using smooth hourglass specimens and a diameteral strain gage. The gage, shown in Figure
6, measures transverse strain which was converted to axial strain with
the use of an analog computer (16). The elevated temperature tests were
essentially the same was before with the exception of the static creep
tests performed. These were done by applying various constant tensile
loads of 40, 50, and 60 Ksi over a 120 second hold time while plotting
strain response versus time.

Notched specimens were subjected to symmetric load patterns with hold times of 100 seconds and a 20 second ramp between tensile and compressive peaks, Figure 5. Again, load and strain data were recorded on

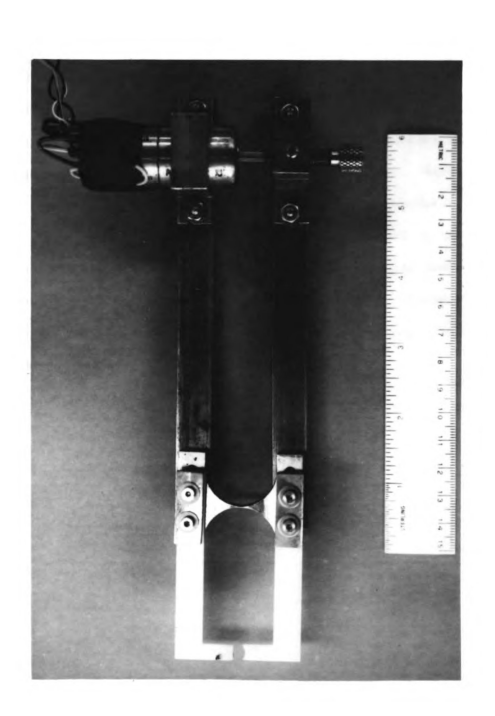


FIGURE 6 DIAMETRAL EXTENSOMETER

1

3 .

b

t

m

3

3.4 SMOOTH SPECIMEN STRESS SIMULATION

In order to determine the stress reponse from the notch root strain histories of the notched specimens, the recorded strains were played back onto smooth specimens. Graphs with the strain data from the notched specimens were placed on the dual pen recorder with one channel connected to the strain output of the extensometer. Stress response of the smooth specimen was hooked to the second channel. The system was set for strain control and a time sweep was started on the plotter. By manually following the strain history of the notched members, the stress response was determined and plotted out. On a second X-Y recorder, stress versus strain plots were also taken. Lucas (16) discusses this method in more detail.

CHAPTER 4

ANALYSIS

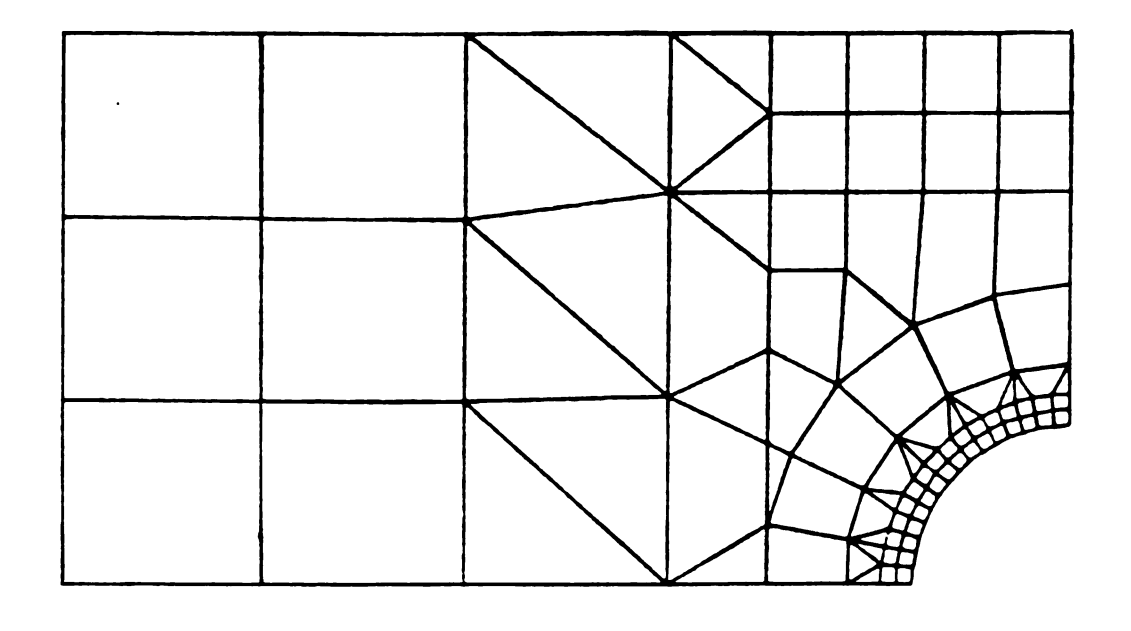
4.1 ANALYTICAL METHODS

Analytical methods used in this study employed a finite element analysis with ANSYS, which is a large scale general purpose program. ANSYS, designed for use on the digitial computer, has been developed, maintained, and advanced by Swanson Analysis Systems Inc (19), ANSYS was utilized on a Prime 750 computer system linked to Tektronix interactive graphics terminals.

The objective of this analysis was to first create 2-D geometric computer models to represent the elliptical and the circular notched specimens. Because of symmetry, it was possible to reduce the models to the quarter section representations shown in Figure 7.

A general rule that was followed was to use quadrilateral elements whenever possible and using triangular elements, when necessary, to model the transition reigons between fine and coarse grids. Finer grids were used where high stress gradients prevailed. Triangular elements have been shown to be less accurate than quadrilaterals of equivalent size and should not be used in high stressed areas unless used in a fine mesh (19).

With the extensive capabilities that ANSYS has, enormous amounts of data were generated for later processing. The memory required to store these data increased dramatically as the number of elements in the model



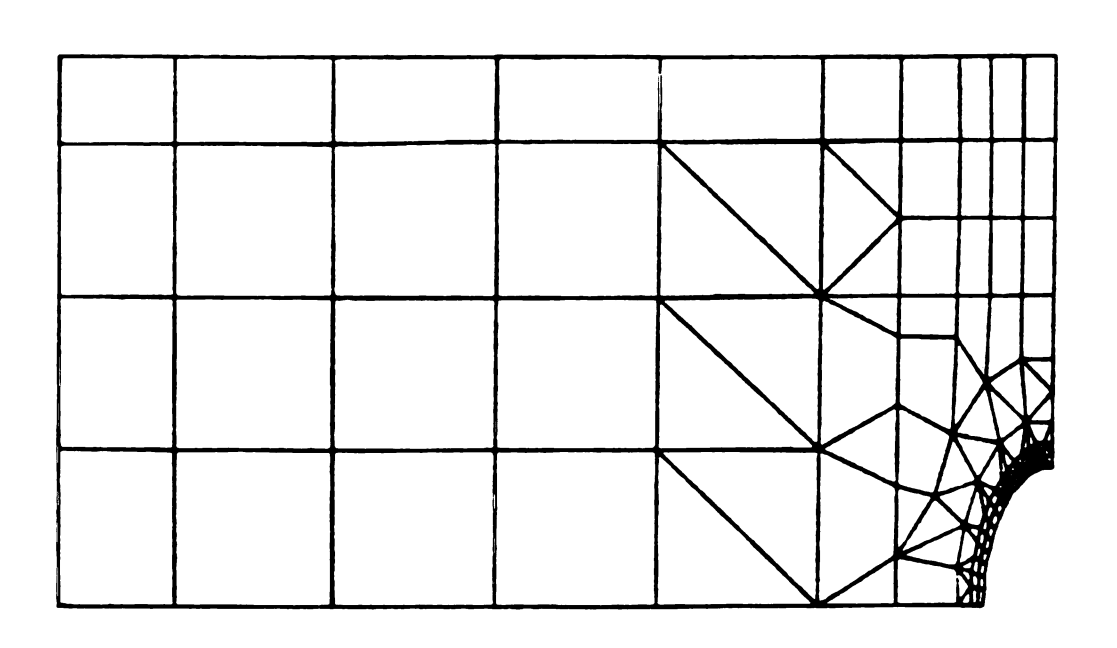


FIGURE 7 FINITE ELEMENT GRIDS

increased thus posing a potential problem to users on smaller systems such as the Prime 750.

The original models developed consisted of over 300 elements and gave good theoretical elastic results. However, an analysis taking plastic effects into account showed that available disk memory was not sufficient to accomadate even two stress reversals. Because of this, the models were reduced down to approximately 100 elements, Figure 7.

Modeling for the circular notch was relatively straight forward. Modeling the ellipse was somewhat more difficult, however, when trying to maintain reasonable aspect ratios with a limited number of elements. Triangles that were used in the finer portion of the mesh helped to alleviate this problem. In order to maintain as much consistiency as possible, the grids for both geometries were modeled in a very similar fashion. A simple four element axisymmetric model was also created in order to look at the predicted stress-strain response of the smooth axial and hourglass specimens. Figure 8 shows a diagram of the model along with its boundary conditions imposed.

The two dimenional isoparametric solid element that was employed here is shown in Figure 9. This element is used for 2-D modeling of solid structures and is capable of being used as a biaxial plane element (plane stress). Both four node and eight node options were available for this element however it was suggested that nonlinear problems could be better solved with a fine mesh that was made of simpler elements as opposed to a more coarse mesh made of higher order elements (19).

ANSYS has an option to include extra displacment shape functions that permits the elements to deform in a parabolic fashion. This is usually a desired effect however interelement incompatability can result

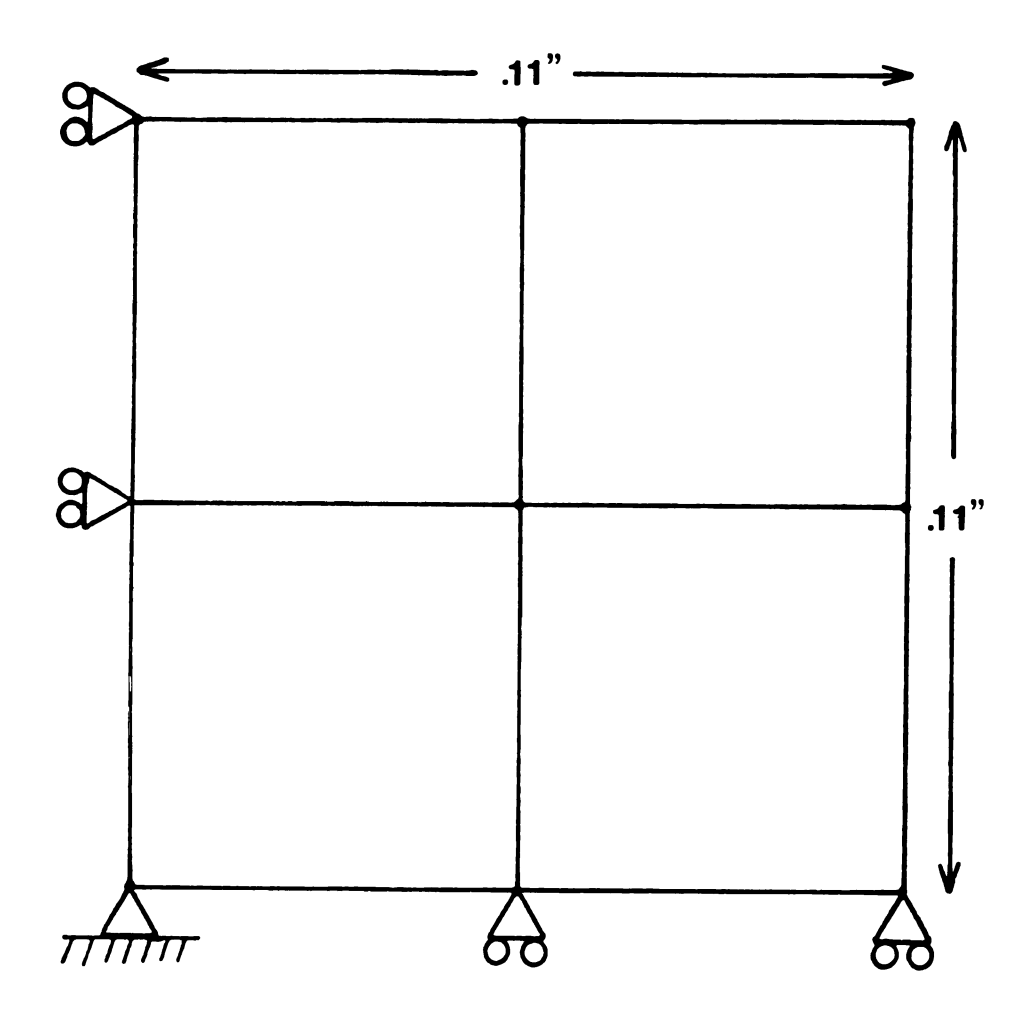


FIGURE 8 AXISYMMETRIC FINITE ELEMENT REPRESENTATION

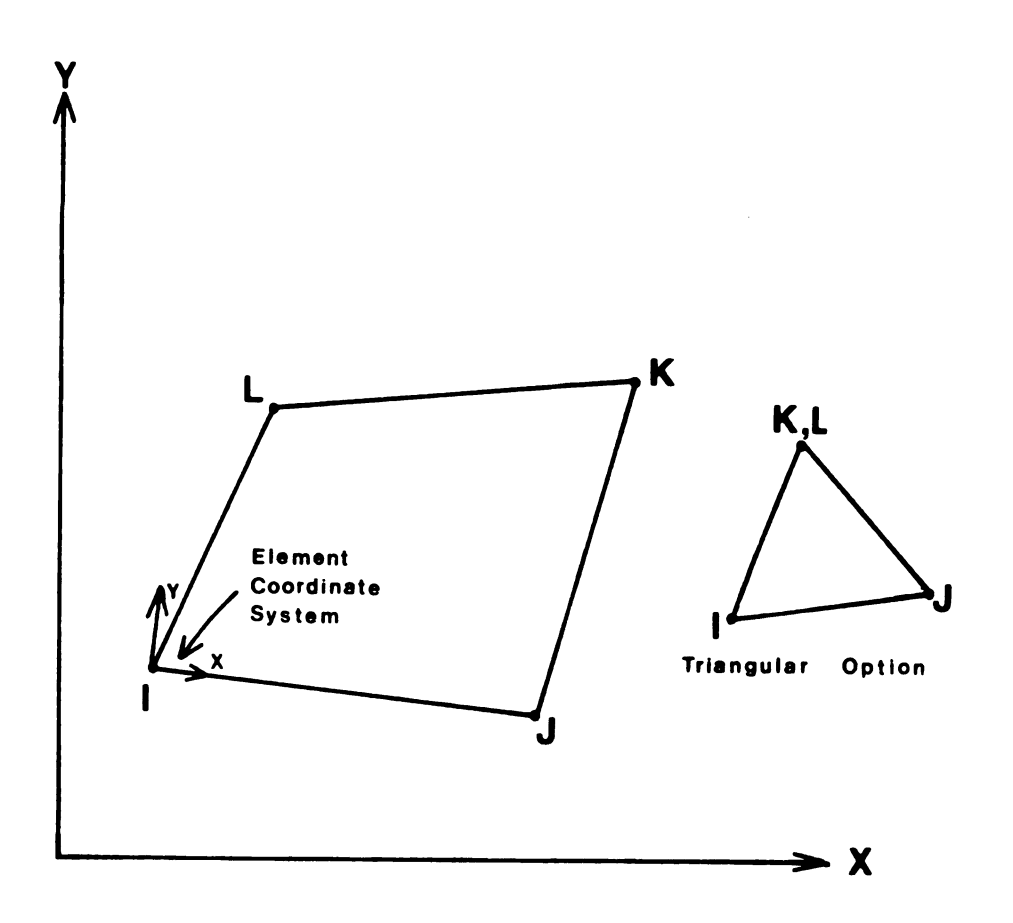


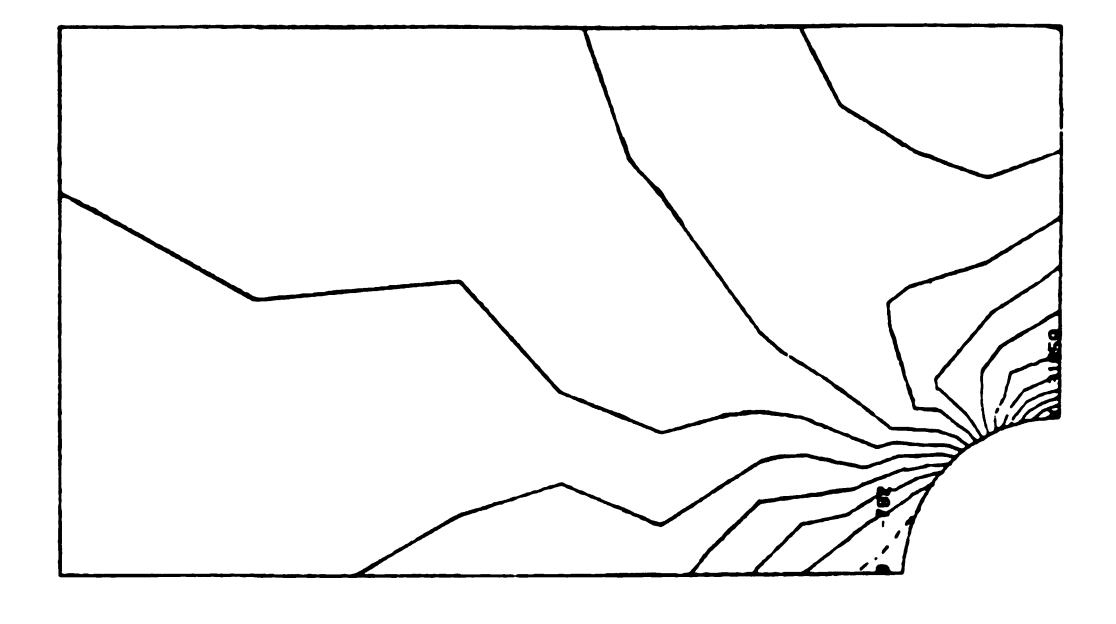
FIGURE 9 TWO DIMENSIONAL ISOPARAMETRIC ELEMENT

at the adjoining edges of different element types such as a gap opening up. Triangular elements cannot accommodate higher order displacements. Because the grids were made up of both triangular and quadrilateral elements, the extra shape option was excluded to avoid incompatability problems. It is also suggested that if the user knows that the element edge deforms linearly, no advantage results from the use of the extra shapes (19).

4.1.1 ELASTIC ANALYSIS

After developing the grids for each of the notch configurations, analyses were made considering only elastic deformation. The results were compared with Peterson (14) for the stress concentrations at the notch. Boundary conditions were imposed on the models by constraining the nodes lying on midchord and midspan lines to deform only along those respective lines. A uniform tensile stress of 10 Ksi was applied along the top horizontal edge of each model in the positive y direction. After computer implementation, the maximum stress resulting at the notch was then compared to Peterson's theoretical values by taking K_{tg} to be $\sigma_{max}/10$ ksi. Post processing of the solution data gave tabulated nodal stresses and displacements as well as interactive graphics plots. Figure 10 shows the σ_y contour plots and Figure 11 shows the displacement plots for the notched models.

For the circular notch, ANSYS showed a K_{tg} of 3.19 which was within 4.0 percent of Petersons' value and the elliptical analysis gave a value of 5.10 for K_{tg} being within 3.9 percent of Peterson. More accuracy could have been attained had finer grid patterns been used however earlier work with this problem showed that disk storage became a problem



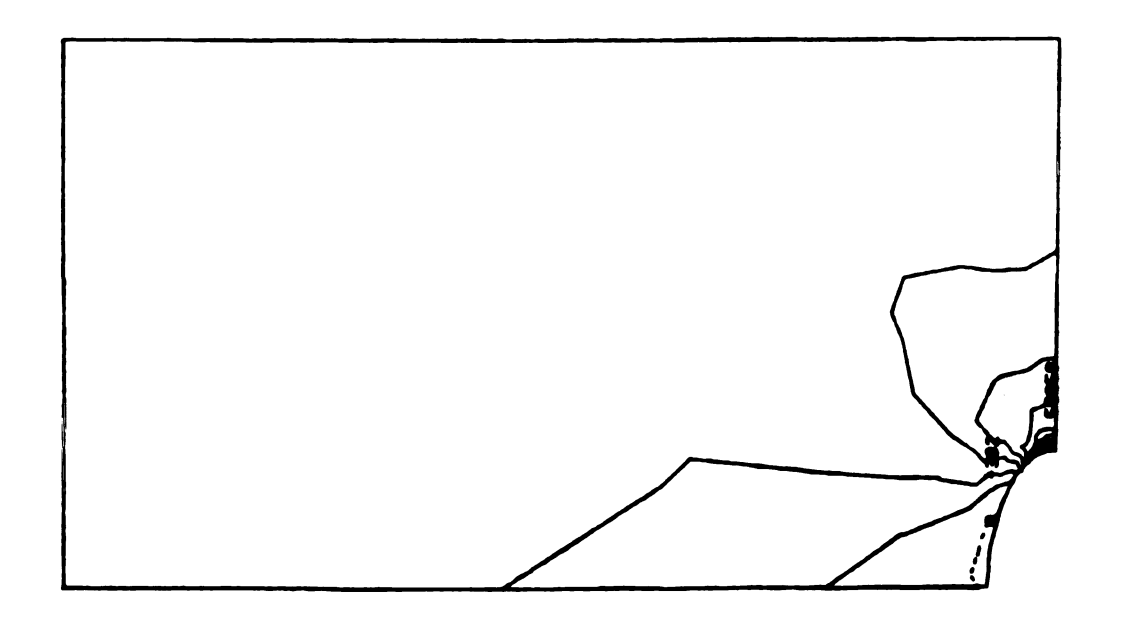
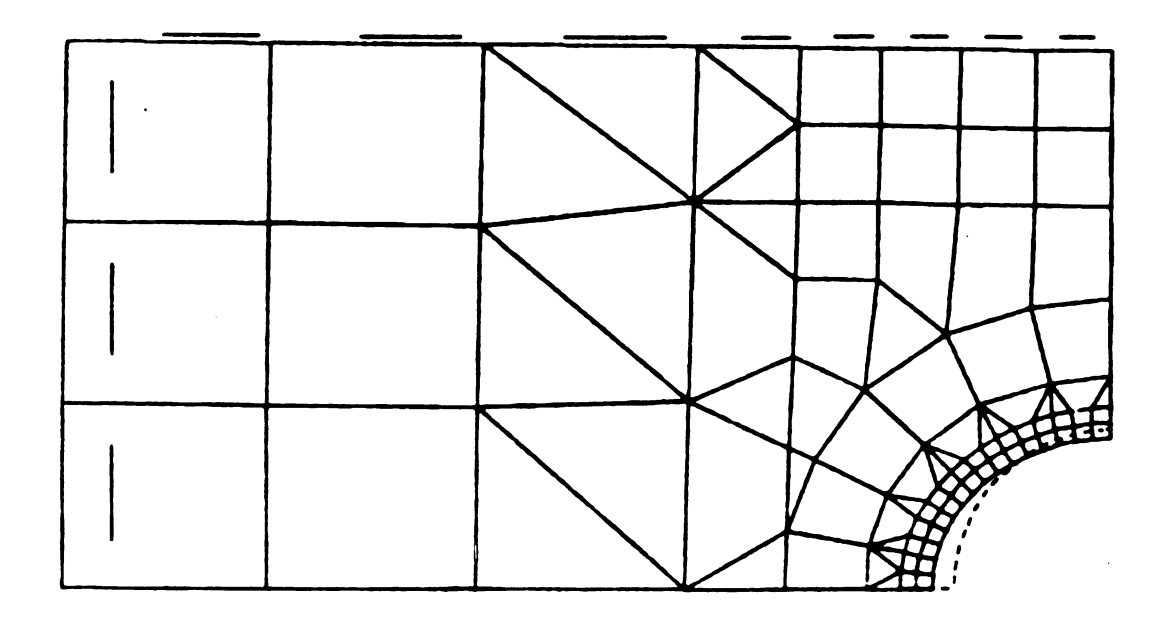


FIGURE 10 ANSYS $\sigma_{\mathbf{y}}$ CONTOUR PLOTS



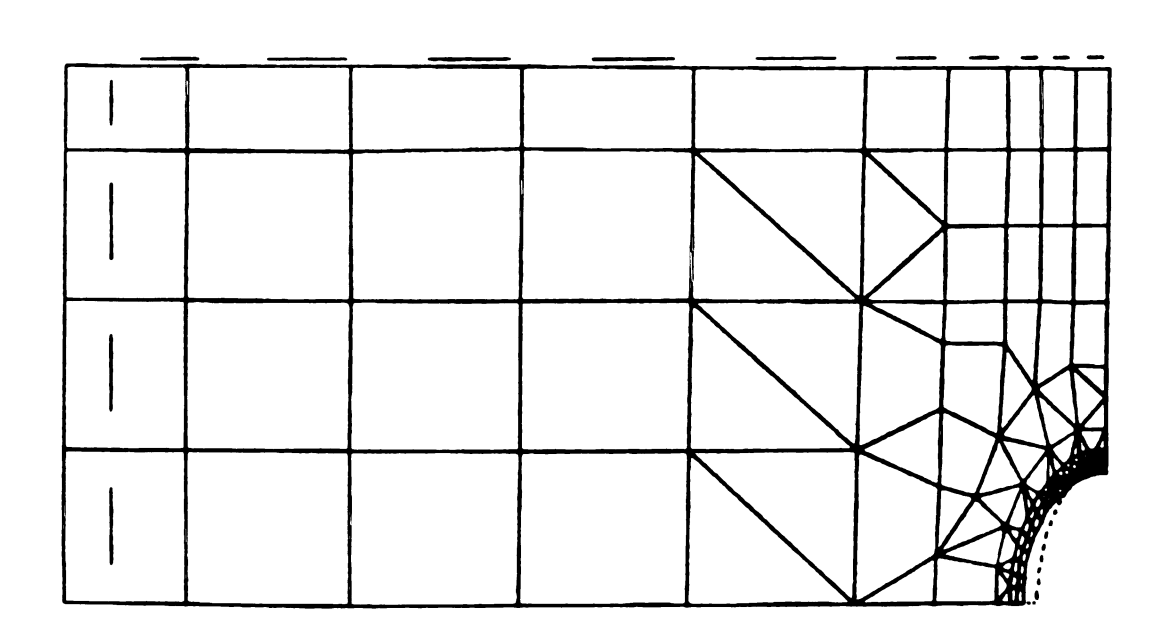


FIGURE 11 ANSYS DISPLACEMENT PLOTS

when using ANSYS in the plastic region due to the large number of iterations required for the solution. For this reason, coarser grids than may have been desired had to be used to facilitate use of ANSYS on the Prime 750. Nevertheless, the values were relatively close for the theoretical comparisons but it must be noted that the results in the plasticity and creep solutions might not be as accurate due to the complexity of the solution process within ANSYS.

4.1.2 PLASTIC ANALYSIS

ANSYS uses the initial stress method to analyze plasticity effects. Yielding is governed by the von Mises yield criterion and multiaxial effects are based on the Prandtl-Reuss flow equations (18). Plastic solutions are restricted to isotropic behavior (20).

ANSYS has several hardening rules that are available to the user. It is recommended and has been shown that a bilinear kinematic hardening model gives results that are most consistient with experimental data (5,19,20). This model assumes a total stress range of twice the yield stress $(2\sigma_y)$ as shown in Figure 12. This was used for all of the plastic analyses.

Plastic analysis with finite elements requires that some experimental data be input as part of the program. ANSYS theory uses physical data that can be generated from a simple uniaxial tension test. Input data consisted of reference temperatures, corresponding modulii of elasticity, yield stresses, and the slopes of the plastic portions of the stress strain curves, Figure 13. If the user is working with several temperatures, ANSYS will use interpolation techniques to obtain results at temperatures other than those specified in the data deck. Up

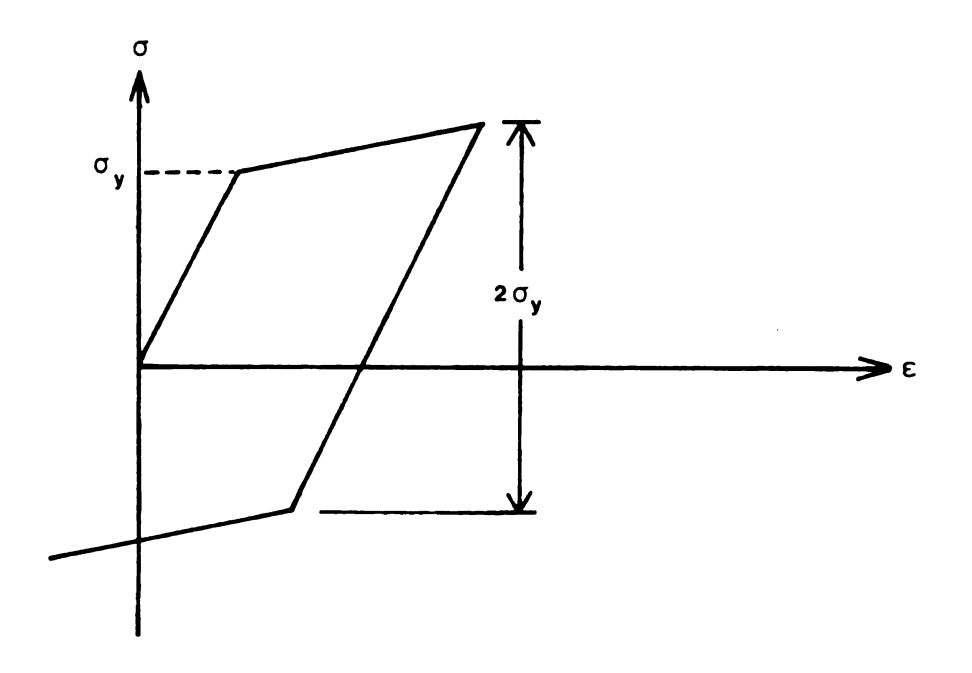


FIGURE 12 BILINEAR KINEMATIC HARDENING MODEL

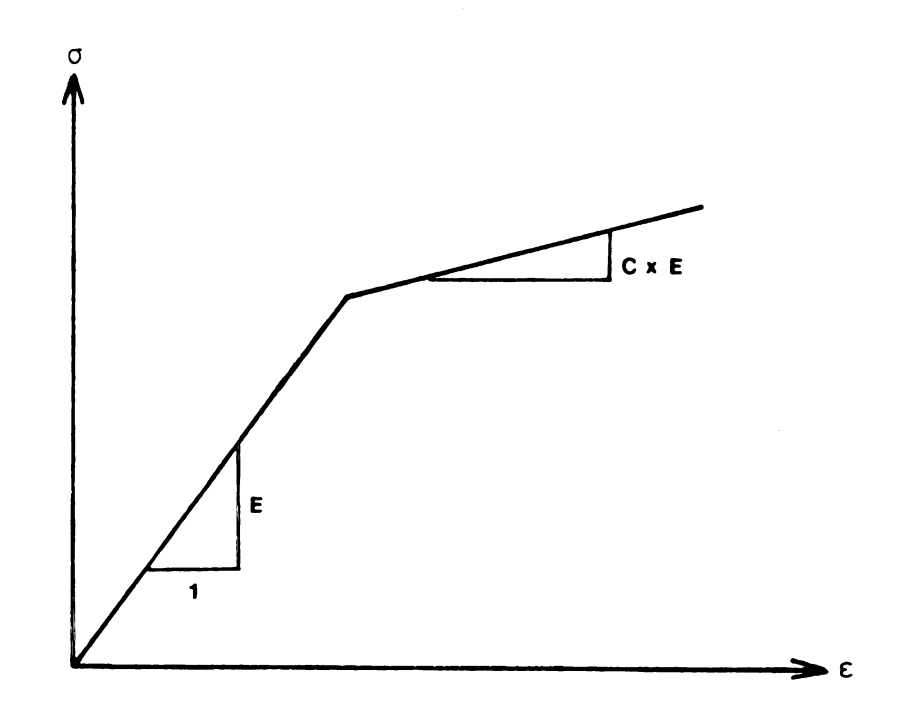


FIGURE 13 BILINEAR FORM OF STRESS-STRAIN RESPONSE

to five temperatures with respective material properties can be entered.

Because this study only deals with two temperatures, these interpolation capabilities were not used and separate data decks were made up for only these temperatures.

In order to maintain a more controlled experimental environment, most of the material properties for ANSYS were determined directly from experimental data generated within this program. Material properties can vary slightly with different batches thus by using data taken from the actual material that was used, this chance of error was reduced. Procedures used to gather these data were discussed in more detail in Chapter 3.

Strain energy concepts were used to determine the plastic slopes of the cyclic stress-strain curves. The shape of these curves were established so that the area enclosed by the models' curve was equal to that of an actual cyclic stress strain loop, Figure 14 (5). With the strain hardening coefficient, n, being determined experimentally in the lab, the slopes are found from the following relation:

SLOPE=
$$(\sigma'/\epsilon'_p)(2n/(1+n))$$
. [3]

It should be noted that this formula does not take into account elastic strains. Yield stresses were also determined from this method, Figure 14, once the corresponding slopes were arrived at.

The classical bilinear kinematic model is a simple and crude method of representing the behavior of a material. Results are highly dependent on the choice of the plastic tangent modulus and the input yield stress. Maximum stress and strain values must be known prior to the

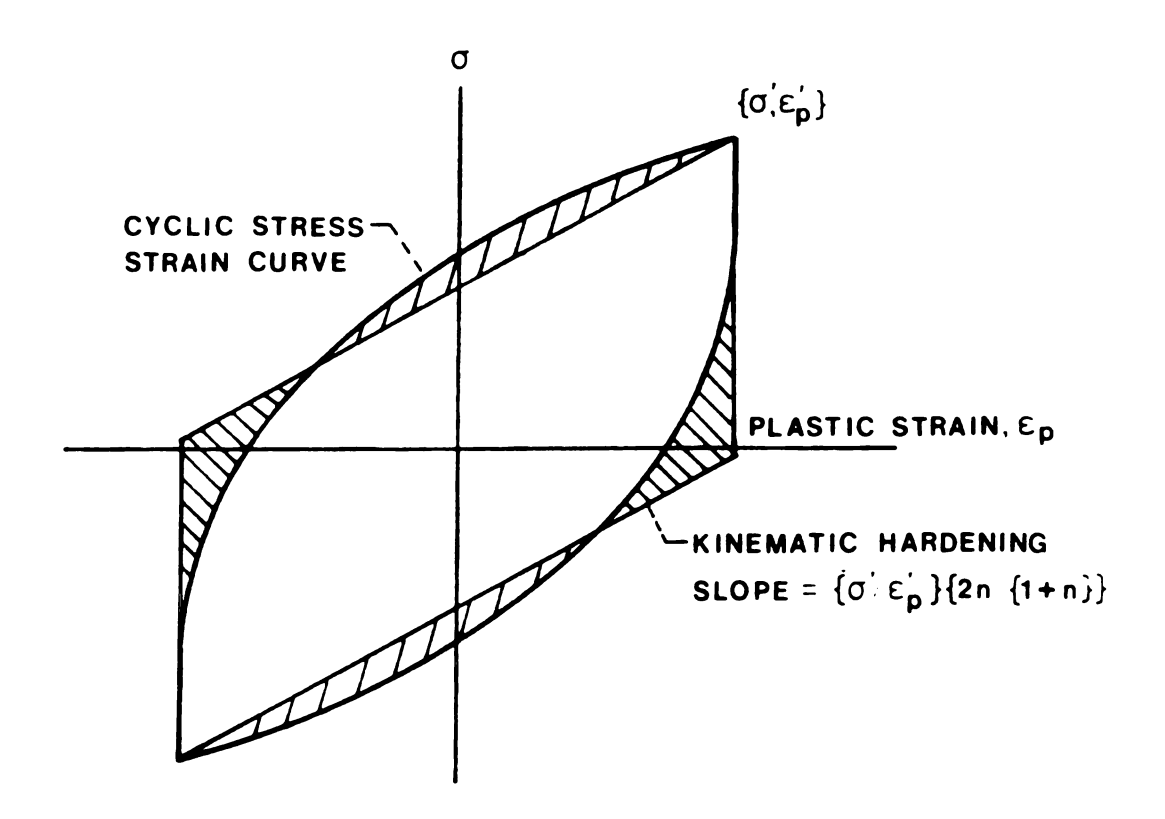


FIGURE 14 STRAIN ENERGY SLOPE DETERMINATION

analysis in order to obtain reliable results. If these values are not predetermined, the solution process can become extremely complicated.

4.1.3 CREEP ANALYSIS

ANSYS solutions that involve creep effects also assume material isotropy. There are many constituitive laws in existience to predict the creep response of materials. Time dependent effects are broken down into three catagories: primary, secondary, and tertiary. Creep tests were described in Chapter 3. Only secondary creep was taken into account for this analytical model. Juvinal (21) discusses secondary creep and gives the following simple equation:

$$\varepsilon_{\text{secondary}} = c_1 \sigma^{C_2} t$$
 [4]

where: t =elapsed time

σ =constant stress applied

Constants C_1 and C_2 were determined from the slopes taken from the creep curves that resulted from isothermal tests performed at three different stresses. Assuming the constants to be the same for all stresses at a given temperature, Equation 4 was manipulated into a form such that linear regression techniques could be used to determine the values for C_1 and C_2 .

Once the constants were obtained, they were entered into ANSYS in a time rate form as follows:

$$\Delta \varepsilon_{\text{secondary}} = C_{1} \sigma^{C} 2 \Delta t$$
 [5]

4.2 COMPUTER IMPLEMENTATION

Uniform stresses were applied at the top horizontal edge of the ANSYS models to simulate loads actually imposed on the laboratory specimens. Assuming that the stress was constant at a sufficient distance from the notch, load schemes were established for the finite element analysis by simply dividing the applied experimental load by the gross cross sectional area of the specimen. These stresses were then applied in several load steps in a gradual manner so as to not allow the ratio of the change in plastic strain $(\Delta \epsilon_{pl})$ to elastic strain (ϵ_{el}) to exceed 3.0 in any given iteration. Allowing this value to exceed 3.0 can result in erroneous answers.

ANSYS will iterate within a load step until the ratio $(\Delta \epsilon_{\rm pl}/\epsilon_{\rm el})$ converges to less than 0.01 unless otherwise specified. This has been described as a fairly tight limit and it was indicated that it could be increased to several percent for most practical problems (19). To reduce computer time and space, all of the ANSYS solutions were run with an assigned value of 0.05 for the convergence criterion.

Computer problems involving creep were set up much like the room temperature ones except time values were also assigned to each of the load steps. These times were determined from the time base load and strain plots obtained in the lab. ANSYS also has a time step optimization option for problems involving creep. The user first selects a reasonable time step. If the option is activated, this time step will be automatically increased within the program thus reducing the number of iterations required for convergence. If the ratio of creep strain to plastic strain exceeds 0.25 in any given iteration, the program will halt and the problem must be initiated again using smaller time steps.

This option was used for all creep analyses in this report (19).

CHAPTER 5

RESULTS AND DISCUSSION

Analytical and experimental results are presented in three sections: linear, nonlinear without creep, and high temperature nonlinear results. For the elastic case, stress distributions across the entire cross section of the specimens were observed, however, only local response at the edge of the notch was considered for the remainder of the report.

5.1 LINEAR ANALYSIS

Experimental results obtained with the ISG were compared with those obtained from ANSYS. For this part of the analysis, the notched specimens were only deformed elastically, Values for K_{tg} could be directly computed from the strain response at the various locations on the specimens. Data were also taken from tests performed by Lucas (16). Nodal stresses along the bottom horizontal edge of the finite element quarter section models divided by the applied gross section stress gave the analytical stress concentrations along the cross sections that were relative to the distance from the edge of the notch.

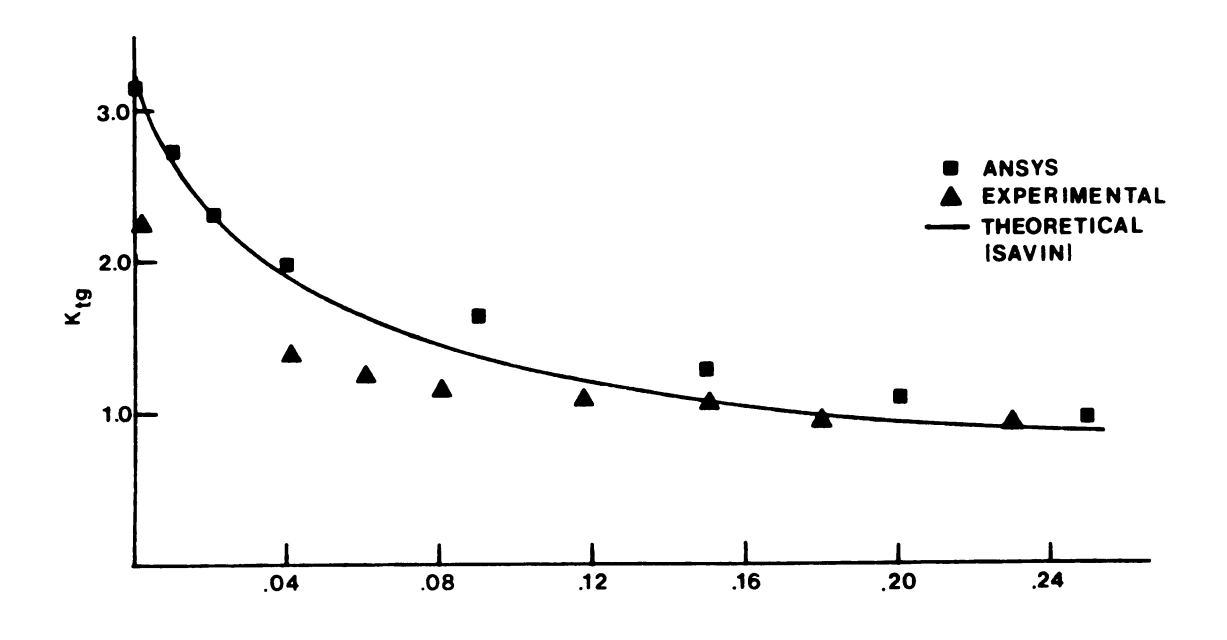
A theoretical stress distribution for the circular notch was taken from Savin (22), however the mathematical solution for the stress distribution in an elliptic notched specimen was somewhat more complicated and could not be found for our particular geometry. These results were

then plotted as K_{tg} versus the distance from the edge of the notch. Figure 15 shows these results. Note that the solid line represents the solution by Savin for the circular geometry and the best fit curve from ANSYS for the elliptical geometry

Correlation of the results between ANSYS and Savin for the circular geometry are shown to be quite good. The values are very close to one another near the notch with a maximum difference of about 15% at the outer edge of the specimen. ISG data, however, proved to have significantly lower K_{tg} values near the notch. At a location 50 microns from the notch, the ISG K_{tg} was about 28% lower than Savin and ANSYS. This variance did reduce however at points that were distant from the notch.

ISG values for the elliptical geometry followed a similar pattern as with the circular specimen but showed an even greater difference from the finite element results. Near the edge of the notch, the error was about 35%. It was noted that the stress gradient was much steeper near the notch of the elliptical specimen as compared to the circular one. Because a theoretical K_{tg} distribution was not available for the elliptical geometry, it is difficult to say just how far off these values are from being mathematicaly correct.

These results are in agreement with Bofferding (17). His work also showed the stress concentrations to be experimentally lower for the notched specimens than what was mathematically predicted. Bofferding's tests also indicated material properties playing a role in how much the experimental stress concentrations varied from the theoretical values.



DISTANCE FROM EDGE OF NOTCH (in)
CIRCULAR GEOMETRY

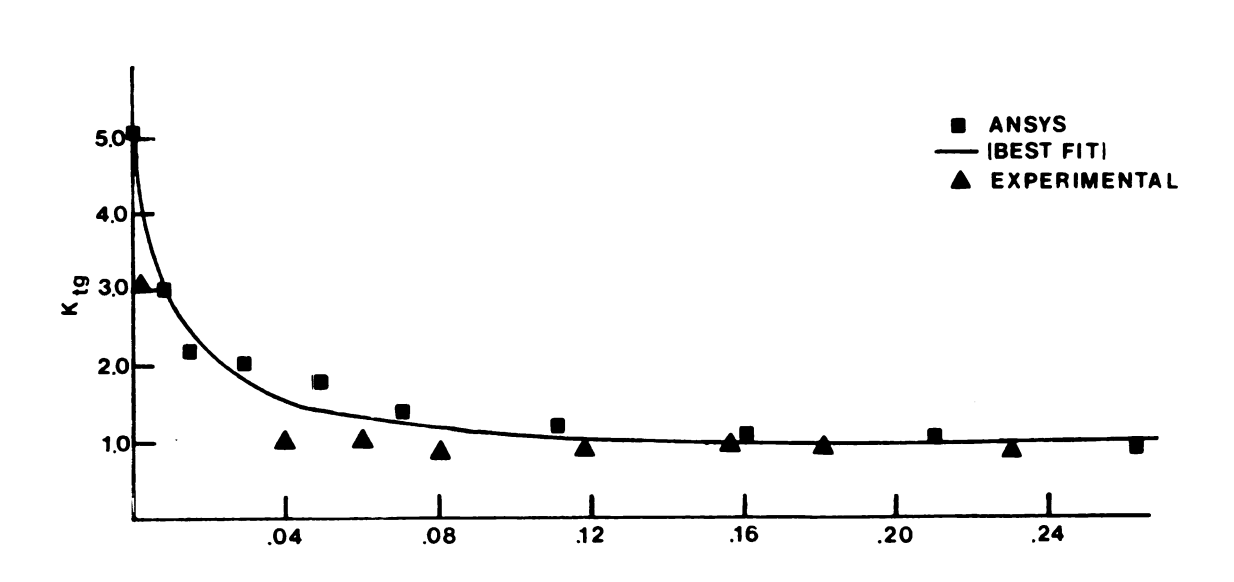


FIGURE 15 STRESS CONCENTRATION PROFILES OF NOTCHED SPECIMENS

DISTANCE FROM EDGE OF NOTCH (in)
ELLIPTICAL GEOMETRY

5.2 NONLINEAR ANALYSIS

The remaining portion of this report consists of analysis of both smooth and notched specimens experiencing deformation into the plastic range. Data are presented graphically in the form of strain versus time and stress versus strain plots. Comparison of analytical and experimental data are done on the same figure for each respective test. Because of the simplicity of the bilinear kinematic model, only the peak stress and strain values are of major interest thus prediction of these peak values will be the main concern in the following discussion.

5.2.1 ROOM TEMPERATURE

The initial results taken from ANSYS examined the stress-strain predictions of a smooth specimen of Hastelloy X. Figure 16 shows the room temperature experimental results and compares them to those from ANSYS. The ANSYS axisymmetric model predicted the response very well with the maximum tensile and compressive peaks being within 5% of the experimental peaks.

For notched geometries, the finite element predictions of notch root strain response versus time was in very good agreement with experimental values for both elliptical and circular geometries. Figures 17 and 18 show these results. Stress-strain results, Figures 19 and 20, are also in good agreement. Notch stresses were simulated with smooth specimens, Chapter 3. Stress values from ANSYS tended to be in more variance from those observed experimentally.

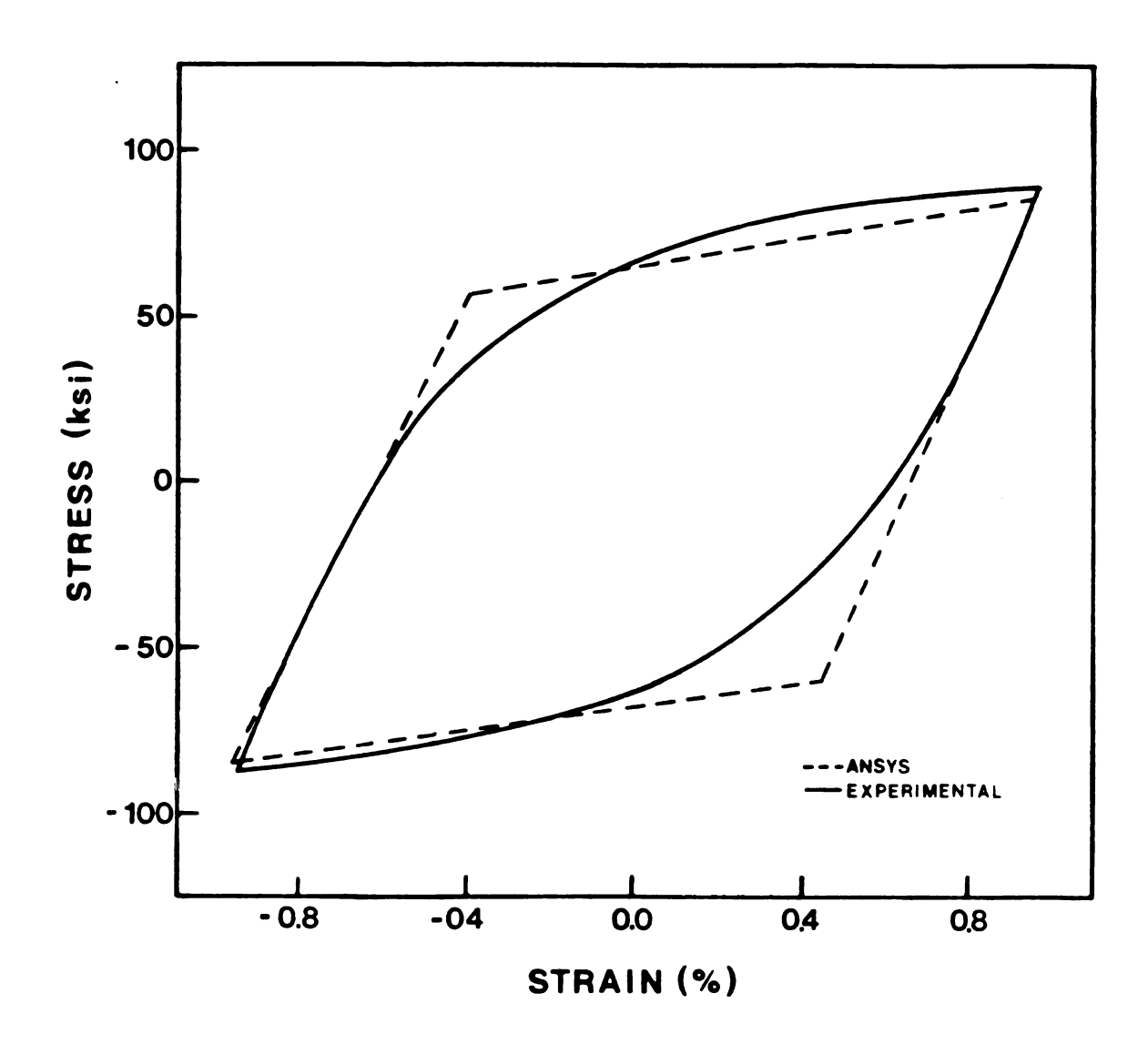
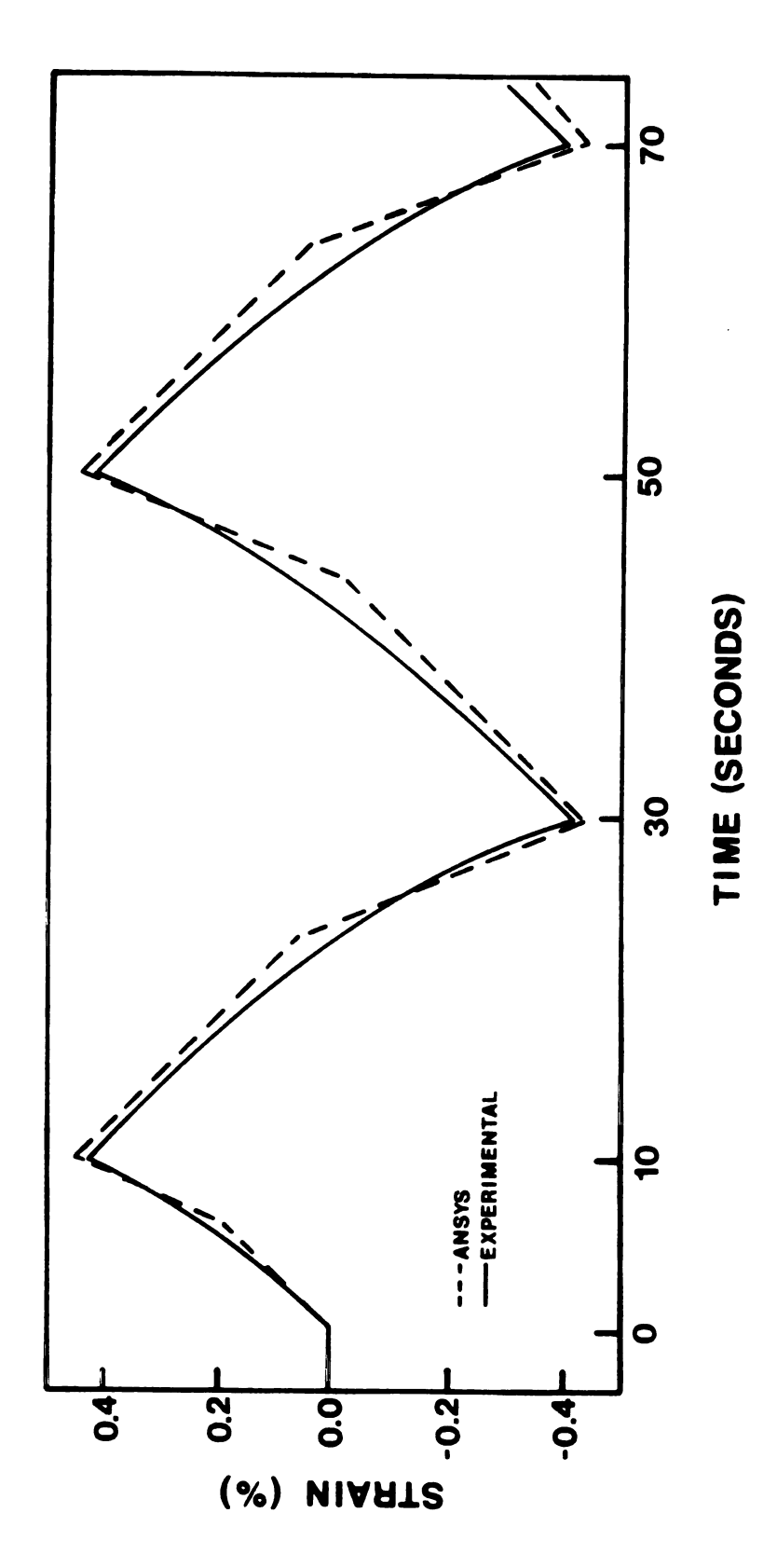
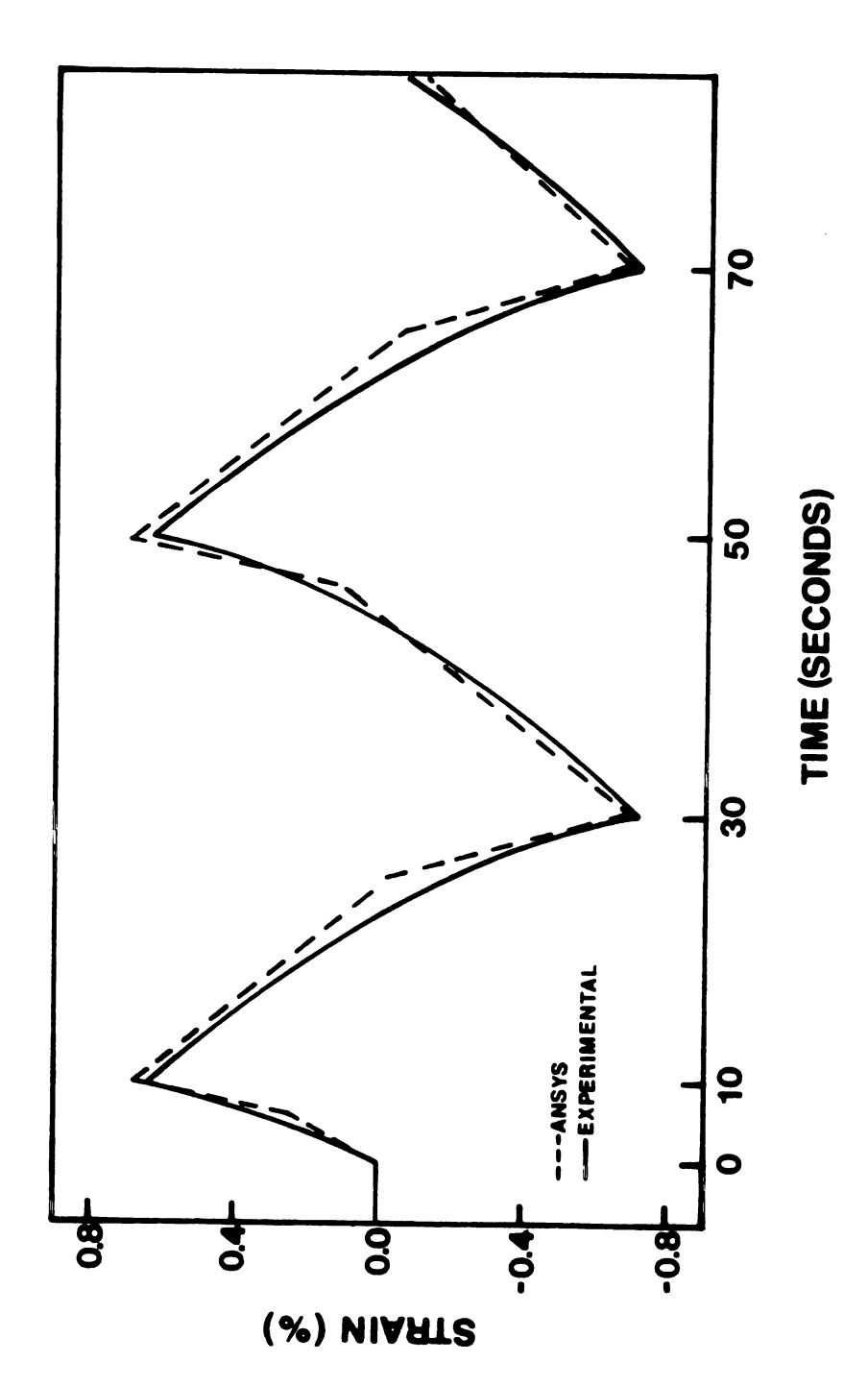


FIGURE 16 HYSTERESIS LOOPS OF SMOOTH SPECIMEN AT ROOM TEMPERATURE



CIRCULAR NOTCH STRAIN VERSUS TIME AT ROOM TEMPERATURE FIGURE 17



ELLIPTICAL NOTCH STRAIN VERSUS TIME AT ROOM TEMPERATURE FIGURE 18

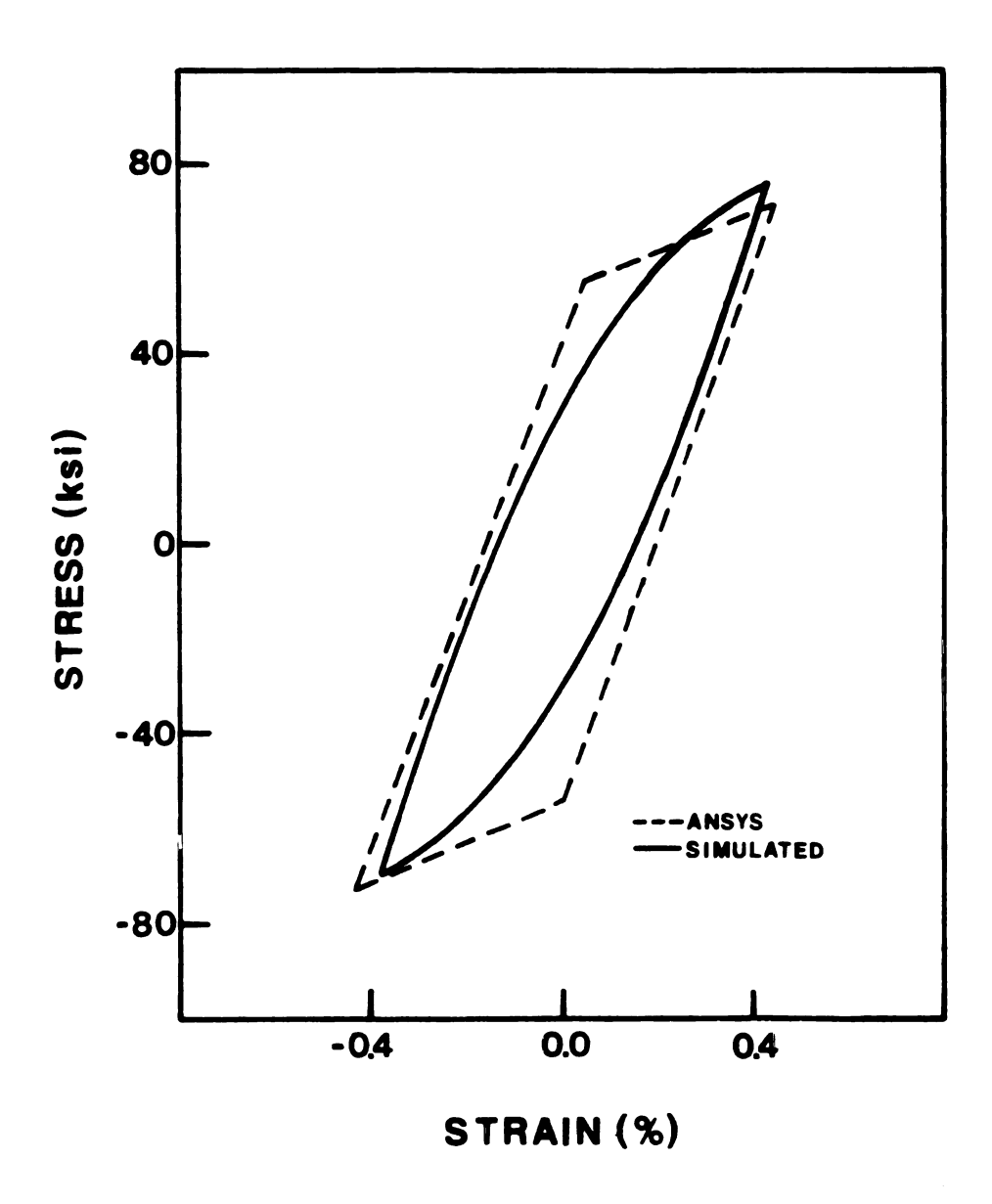


FIGURE 19 STRESS VERSUS STRAIN OF CIRCULAR NOTCHED SPECIMEN AT ROOM TEMPERATURE

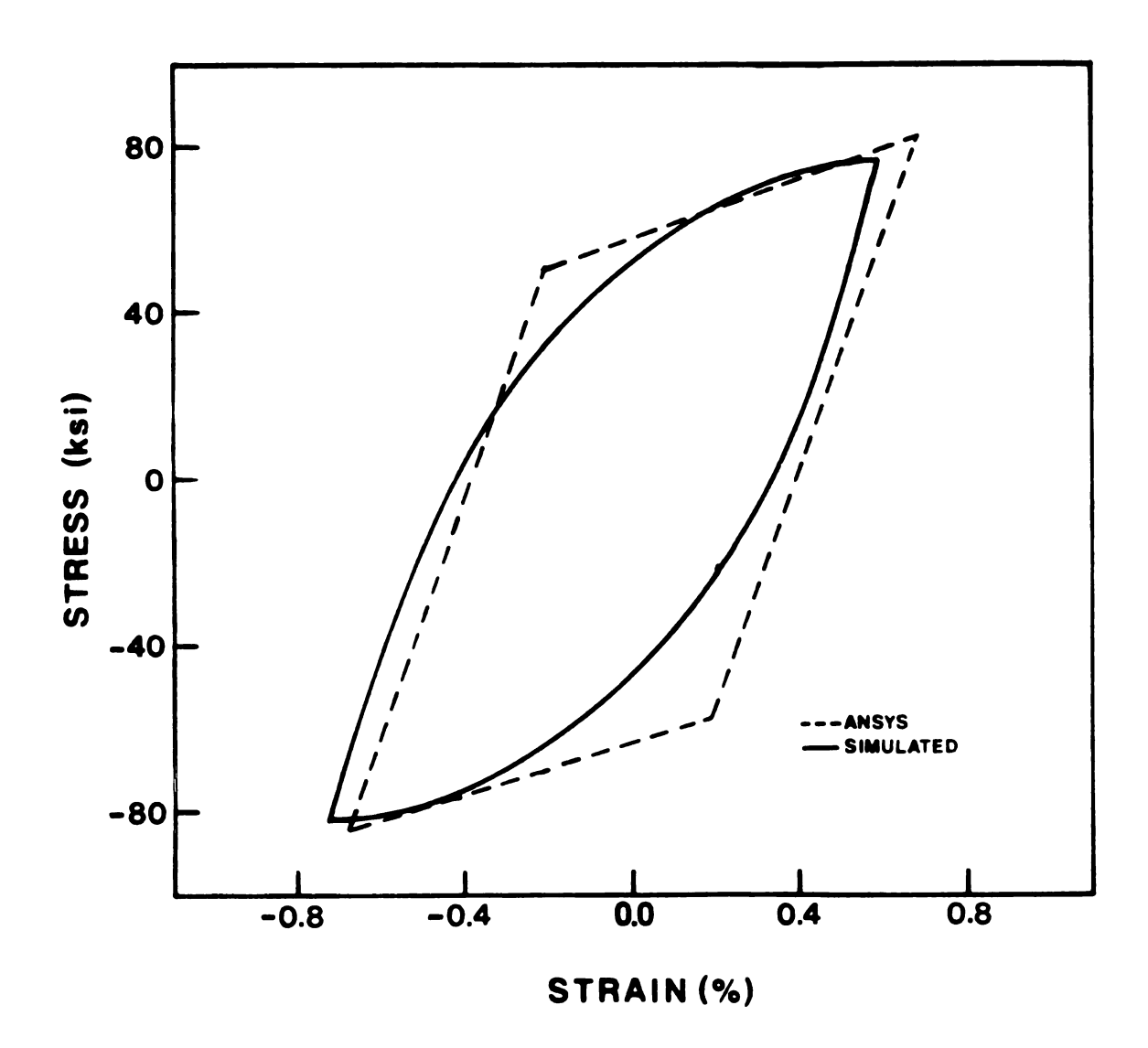


FIGURE 20 STRESS VERSUS STRAIN OF ELLIPTICAL NOTCHED SPECIMEN AT ROOM TEMPERATURE

5.2.2 ELEVATED TEMPERATURE

As before with the room temperature tests, a simple stress-strain prediction with the axisymmetric finite element model was performed. All tests and analyses were for an isothermal temperature of 1,200° F. Figure 21 shows results for smooth specimens. Agreement was not as close as the room temperature results. The tensile peak was in good agreement however the compressive peak varied about 15%. This non-symmetric behavior of Hastelloy X is much more predominant at higher temperatures making predictions with a bilinear model, which assumes a symmetric response, more difficult.

ANSYS creep predictions for a smooth specimen under constant stress are compared to the experimental curves used to determine the creep constants, Figure 22. Analytical curves were lower for each case due to the fact that primary creep was not taken into account.

Notch root strain-time prediction gave relatively poor results in comparison to the room temperature results. As seen in Figure 23, the general shape of the curves are the same for the strain-time response but the peaks are significantly lower than those from the experimental results. Stress-strain predictions, Figure 24, were also poor, however, the peak stress values were reasonably close to those simulated on smooth specimens in the lab. Note the nonsymmetric behavior that ANSYS predicts when a creep model is used in the analysis. Due to the fact that the stress range is $2\sigma_y$, added creep strain causes the model to deform less in compression than in tension for this particular load history.

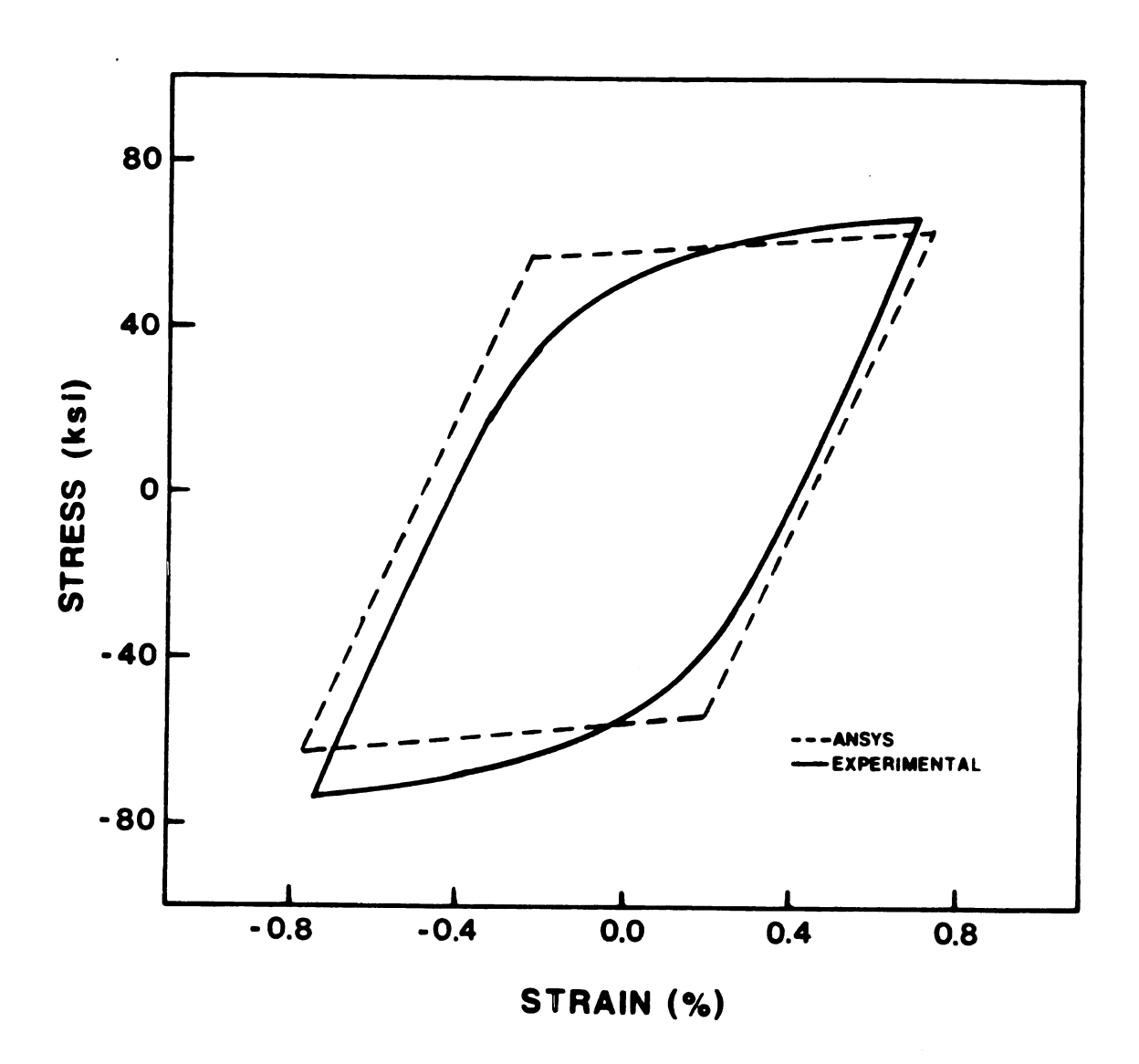


FIGURE 21 HYSTERESIS LOOPS OF SMOOTH SPECIMEN AT $1,200^{\circ}$ F

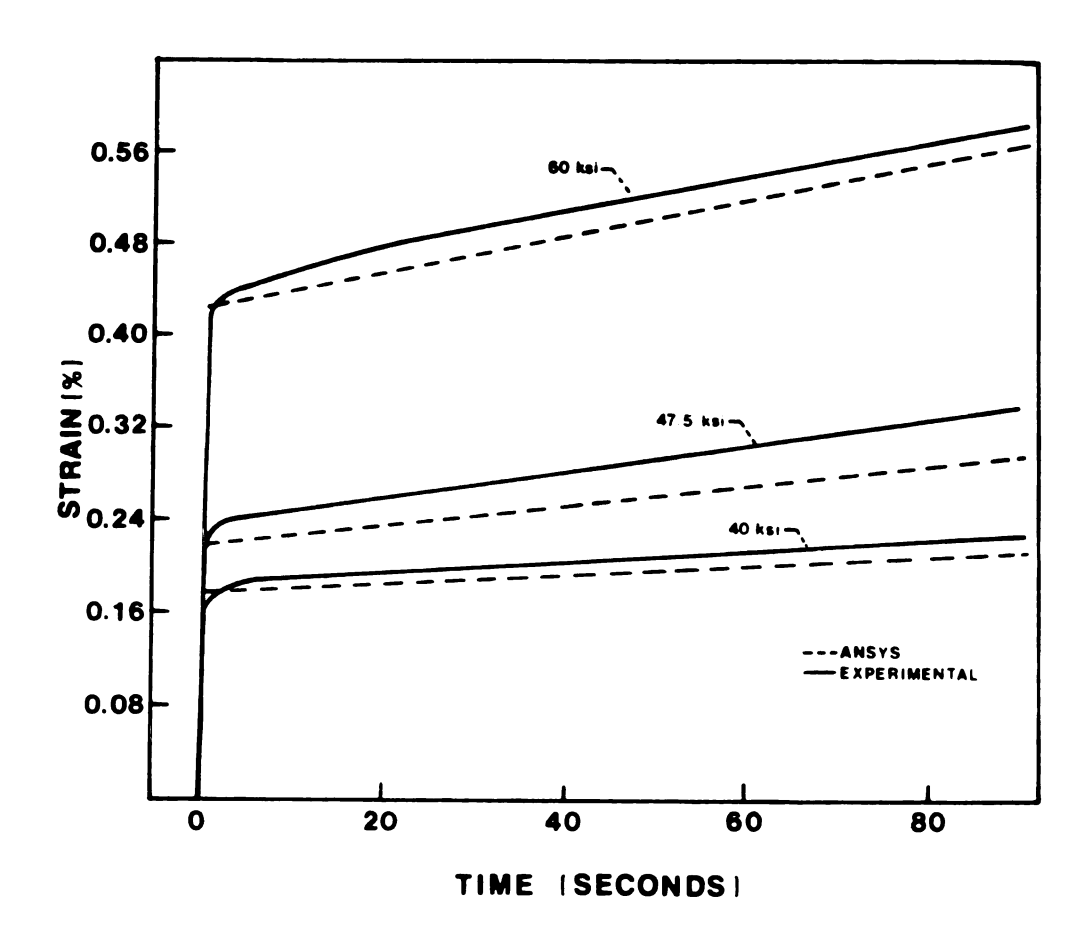
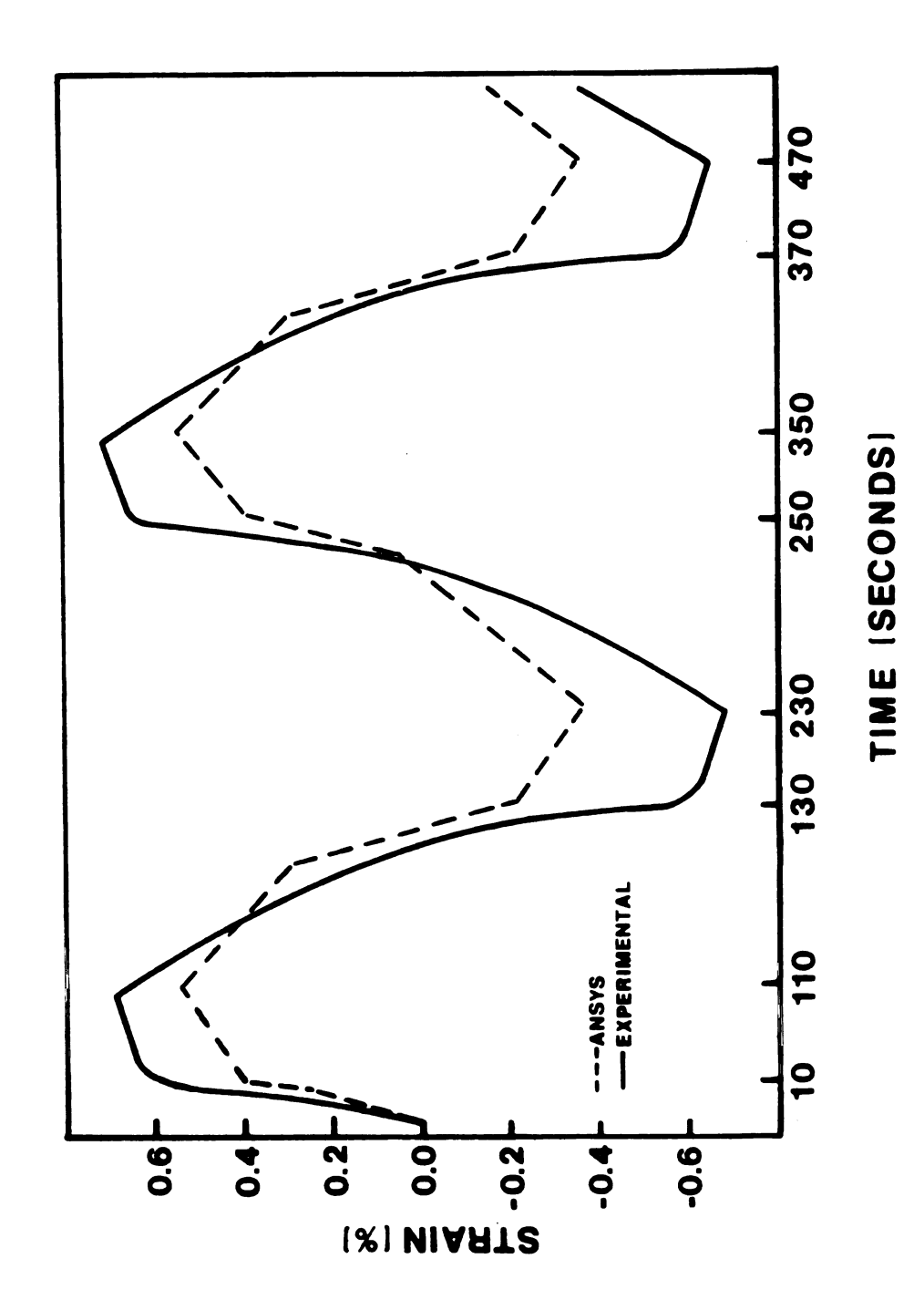


FIGURE 22 CREEP RESPONSE OF SMOOTH SPECIMEN UNDER CONSTANT STRESS AT 1,200° F



STRAIN VERSUS TIME OF CIRCULAR NOTCHED SPECIMEN AT 1,200° F FIGURE 23

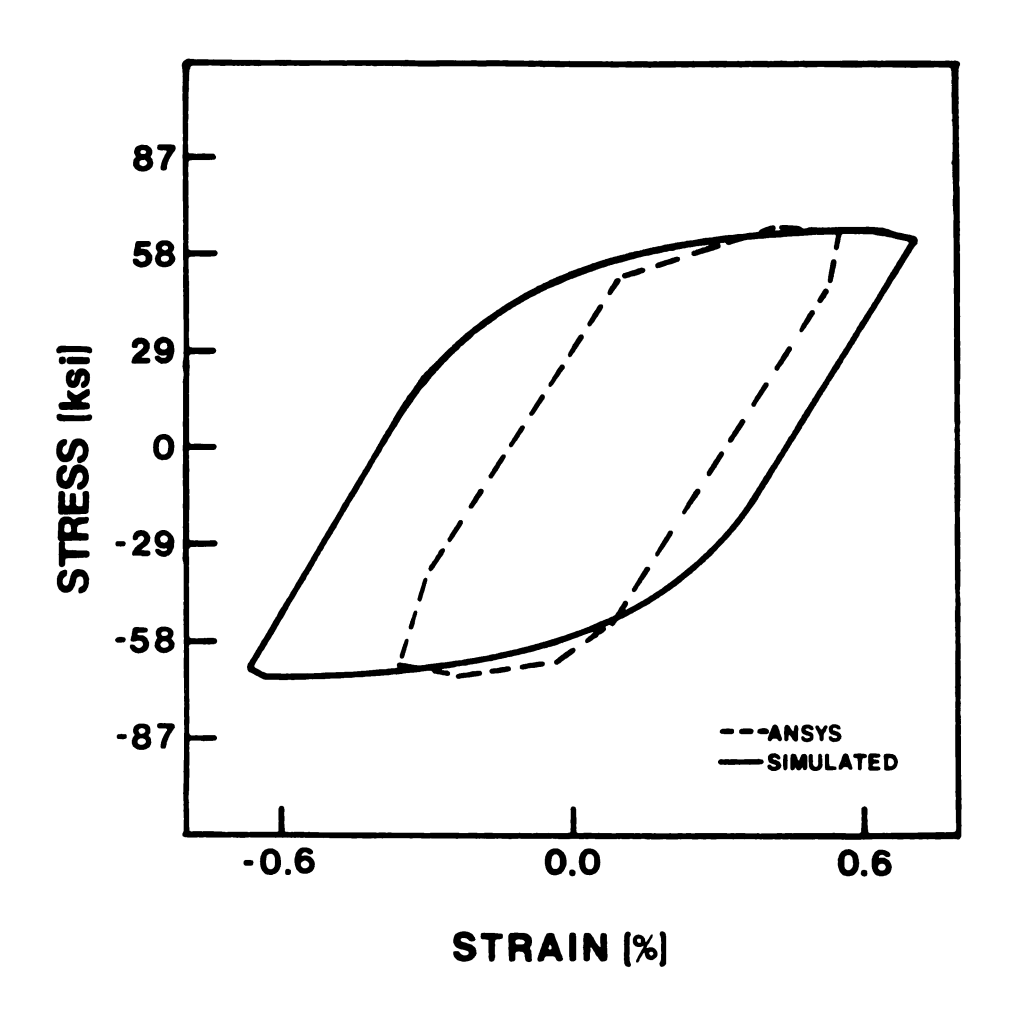


FIGURE 24 STRESS VERSUS STRAIN OF CIRCULAR NOTCHED SPECIMEN AT 1,200° F

CHAPTER 6

CONCLUSIONS

Finite element prediction of notch root stress-strain response behavior using ANSYS gave very good results in comparison to the experimental values for both geometries at room temperature. Strain response, in particular, was very accurate for these tests.

Analytical values for stress concentration factors in the elastic range were consistently higher than experimental results from both geometric cases. Variance between theoretical and experimental K_{tg} values were greater for the elliptical than the circular notch.

Predicted notch root stress-strain response at 1,200° F for the circular geometry was poor in comparison to experimental behavior.

Analytical peaks were significantly less in both tension and compression with maximum error ranging to 40% on the compressive side.



LIST OF REFERENCES

- 1. National Aeronautics and Space Administration, "Turbine Engine Hot Section Technology(HOST), "NASA Technical Memorandum 83002, October, 1982, pp. 1-3, pp. 45-53.
- 2. United Technologies, Pratt and Whitney Aircraft, "3D Inelastic Analysis Methods for Hot Section Components," Technical Proposal No. 82-4059, August, 1982.
- 3. Walker, K. P., "Research and Development Program for Nonlinear Structural Modeling with Advanced Time-Temperature Dependent Constitutive Relationships," NASA Report No. CR-165533, November, 1981.
- 4. Kaufman, A., "Evaluation of Inelastic Constitutive Models for Nonlinear Structural Analysis," NASA Technical Memorandum 82845, May, 1982.
- 5. Drake, S. K., Hill, R. J., Kladden, J. L., "Three Dimensional Finite-Element Elastic Analysis of a Thermally Cycled Double-Edge Wedge Geometry Specimen," Technical Report AFWAL-TR-80-2013, Wright-Patterson Air Force Base, Dayton, Ohio, January, 1979.
- 6. Sharpe, W. N., Jr., "The Interferometric Strain Gage," Experimental Mechanics, Vol. 8, No. 4, April, 1968, pp. 164-170.
- 7. Sharpe, W. N., Jr., "Interferometric Surface Strain Measurement,"

 International Journal of Non-Destructive Testing, 3, 1971, pp.

 51-76.
- 8. Sharpe, W. N., Jr., "A Short Gage Length Optical Gage for Small Strain," Experimental Mechanics, Vol. 14, No. 9, 1974, pp. 373-377.
- 9. Sharpe, W. N., Jr., "Development and Application of an Interferometric System for measuring Crack Displacements," Final Report on Grant NSG 1148, June, 1976.
- 10. Crews, J. H., Jr., and Hardrath, H. F., "A Study of Cyclic Plastic Stresses at a Notch Root," <u>Experimental Mechanics</u>, Vol. 6, No. 6, June, 1966, pp. 313-320.

- 11. Wetzel, R. M., "Smooth Specimen Simulation of Fatigue Behavior of Notches," <u>Journal of Materials</u>, JMLSA, Vol. 3, No. 3, September, 1968, pp. 646-657.
- 12. Lies, B. N., Gowda, C. V. B., and Topper, T. H., "Cyclic Inelastic Deformation and the Fatigue Notch Factor," ASTM STP 519, American Society for Testing and Materials, 1973, pp. 133-150.
- 13. Stadnick, S. J., and Morrow, JoDean, "Techniques for Smooth Specimen Simulation of the Fatigue Behavior of Notched Members," ASTM STP 515, American Society for Testing and Materials, 1972, pp. 229-252.
- 14. Peterson, R. E., "Stress Concentration Factors," John Wiley and Sons, Inc., 1974, pp. 150-196.
- 15. Cabot Corporation, "Hastelloy Alloy X," High Technology Materials Division, June, 1976.
- 16. Lucas, L. J., "Experimental Verification of the Neuber Relation at Room and Elevated Temperatures," Masters Thesis, Michigan State University, 1982.
- 17. Bofferding, C. H., "A Study of Cyclic Stress and Strain Concentration Factors at Notch Roots Throughout Fatigue Life," Masters Thesis, Michigan State University, 1980.
- 18. Mendelson, A., "Plasticity: Theory and Application," The Macmillan Company, 1970, pp. 75-77, 100-104.
- 19. Swanson Analysis Systems Inc., "ANSYS User's Manual," Houston, Pennsylvania.
- 20. Swanson Analysis Systems Inc., "ANSYS Theoretical Manual," Houston, Pennsylvania.
- 21. Juvinall, Robert, C., "Engineering Considerations of Stress, Strain, and Strength," McGraw-Hill Inc., 1967, pp. 410-424.
- 22. Savin, G. N., "Stress Concentration Around Holes," Pergamon Press, 1961, pp. 104-110.

